

Spectroscopy of H_3^+ : planets, chaos and the Universe

Jonathan Tennyson

Department of Physics and Astronomy, University College London, London WC1E 6BT, UK

Abstract

This review discusses the H_3^+ molecular ion and its deuterated isotopomers. The ion is important because of its fundamental nature, astrophysical significance and dynamical richness. The following topics are discussed: the discovery of H_3^+ , its unusual bonding and the important role played by *ab initio* electronic-structure calculations; the formation of H_3^+ and its importance in models of the interstellar medium; the unusual spectroscopy of H_3^+ and the accurate quantum calculations which led to laboratory observations; the failure to detect H_3^+ in the interstellar medium and its accidental observation in Jupiter; work on H_3^+ in the giant planets and other astronomical emission spectra; the very unusual infrared photodissociation spectrum of H_3^+ ; and the classical and quantal behaviour of the molecule at its dissociation limit.

This review was received in December 1994.

Contents

	Page
1. Introduction	424
2. Discovery and structure of H_3^+	425
2.1. Original detection	425
2.2. Structure and stability	425
2.3. Ground-state electronic-structure calculations	426
3. Importance of H_3^+ in the interstellar medium	428
3.1. Nature of the ISM	428
3.2. Formation and destruction of H_3^+	429
3.3. H_2D^+ and deuterium fractionation	430
4. Spectroscopy	432
4.1. Symmetry	432
4.2. Vibration-rotation energy levels	432
4.3. Deuterated species	434
4.4. Nuclear spin effects	435
5. Laboratory spectra of H_3^+	436
5.1. The first detection	436
5.2. Variational calculations	436
5.3. Fundamental, overtone and hot bands of H_3^+	439
5.4. Spectra of deuterated H_3^+	441
5.5. Spectroscopically determined potential energy surfaces	442
6. Attempts to observe H_3^+ in the interstellar medium	445
6.1. Absorption spectra of H_3^+	445
6.2. Attempts to detect H_2D^+ in the ISM	446
7. H_3^+ in Jupiter	447
7.1. Detection	447
7.2. Temperature of H_3^+ emissions	448
7.3. Morphology	450
7.4. Impact of comet Shoemaker-Levy 9	451
8. H_3^+ in the other giant planets	451
8.1. Detection in Uranus	451
8.2. Saturn and Neptune	452
9. H_3^+ in emission outside the solar system	453
9.1. Background	453
9.2. Supernova 1987a	453
9.3. Emissions from other sources	455
10. H_3^+ at its dissociation limit: laboratory spectra	455
10.1. The original observation	455
10.2. Detailed spectrum and its coarse-grained structure	456
10.3. Lifetimes of the states involved	456
10.4. Isotopic substitution	457
10.5. Spectra at high kinetic energy release	457

11. H_3^+ at its dissociation limit: (semi)classical studies	458
11.1. General considerations	458
11.2. Lifetimes	459
11.3. Density of states	460
11.4. Structure of phase space	462
11.5. Angular momentum barriers	463
12. H_3^+ at its dissociation limit: quantal studies	464
12.1. The challenge and early attempts to meet it	464
12.2. Vibrational states at dissociation	465
12.3. Rotational states at dissociation	467
12.4. Of horseshoes and elephants' feet	467
13. Conclusions	471
Acknowledgments	471
References	471

1. Introduction

It is often said that H_3^+ is the simplest polyatomic molecule. It is true that its electronic structure is simple: H_3^+ has only one stable electronic state and no known electronic spectrum. However, the simplicity of H_3^+ 's electronic behaviour is offset by richness in its nuclear dynamics.

H_3^+ is usually formed via the reaction:



which is exothermic by about 1.7 eV. Essentially a reaction occurs every time the hydrogen molecule and its ion collide. This means that H_3^+ is present in any environment where molecular hydrogen gas is ionized.

There are three reasons for the large volume of work that has taken place on H_3^+ over the last decade: its fundamental nature, astrophysical significance and dynamical richness as characterized by its photodissociation spectrum. In this period H_3^+ has been the subject of a number of reviews; notably those by Oka (1992a) and Tennyson and Miller (1994) on the interaction of laboratory and astrophysical spectroscopy, Miller and Tennyson (1992), Dalgarno (1994) and Miller *et al* (1994) on the astrophysics of H_3^+ , Carrington and McNab (1989) and Pollak and Schlier (1989) on the photodissociation spectrum and a comprehensive survey of H_3^+ spectroscopy by McNab (1995).

Development of the theoretical treatments of polyatomic molecules has meant that calculations on H_3^+ , using first-principles quantum mechanics, have achieved accuracies only surpassed by work on molecular hydrogen (Kolos and Wolniewicz 1965). H_3^+ has thus become a benchmark against which theoretical treatments are tested. Unusually also, nearly all the advances made in the spectroscopy of H_3^+ have relied upon *ab initio* quantum mechanics.

As hydrogen is by far the most abundant element in the Universe and molecular hydrogen is known to dominate in cool regions, H_3^+ should be an astrophysically important species. In fact H_3^+ is a vital species in models of the large, cold molecular clouds which occur in the interstellar medium. However, in part at least because of its unusual spectroscopy, H_3^+ has proved elusive exactly where it is thought to be most important but has proved surprisingly easy to observe in other, hotter environments.

My personal interest in the H_3^+ molecular ion was stimulated by a brief research note published by Carrington *et al* (1982). This was a preliminary communication of an extremely unusual photodissociation spectrum



where the energy of the laser photon, $h\nu$, was only a small fraction of the dissociation energy of ground-state H_3^+ . By monitoring protons produced in this process, Carrington *et al* (1982, 1993, Carrington and Kennedy 1984) obtained a very complicated spectrum which, to this day, has defied interpretation in conventional spectroscopic terms.

This review discusses both the astronomy and photodissociation dynamics of H_3^+ . The understanding of both of these are underpinned by conventional high-resolution spectra of

H_3^+ , which also have many unusual features. As a theoretician I will attempt to survey both theoretical and experimental (observational) work on H_3^+ ; but will not aim for a review of experimental methods (which can be found in McNab (1995)). The review begins with a historical overview of H_3^+ and a discussion of its electronic structure, moves onto spectroscopy and then H_3^+ astronomy. The final parts will be devoted to its photodissociation dynamics.

2. Discovery and structure of H_3^+

2.1. Original detection

H_3^+ was originally discovered by J J Thomson (1911, 1912) as part of his further experiments on positive rays⁷. Using a very early version of mass spectroscopy, he identified an ion with a 3:1 mass-to-charge ratio which, after eliminating other possibilities, he concluded could only come from a molecule formed from three hydrogen atoms. He noted that 'the existence of this substance is interesting from a chemical point of view, as it is not possible to reconcile its existence with ordinary conceptions about valency'. However, the discovery of deuterium some 20 years later led many people, including Thomson (1934), to ascribe his observations to HD^+ .

The formation of H_3^+ in hydrogen discharges was studied by Dempster (1916). He showed that as pressure was increased H_3^+ became the dominant ion in preference to either H^+ or H_2^+ . A fuller review of the early work on H_3^+ is given by Oka (1983).

2.2. Structure and stability

Theoretical work on H_3^+ dates from the 1930s when Hirschfelder and co-workers performed a series of electronic-structure calculations. As a closed-shell two-electron system such calculations can be performed accurately and cheaply using modern computers (see below) but in the precomputer era the evaluation of the relevant integrals was a formidable task (see Hirschfelder and Weygandt (1938) for example). These calculations showed conclusively that H_3^+ was not only bound with respect to dissociation into H_2 and a proton but also that the H_3^+ formation reaction (1.1) was exothermic. The calculations had more difficulty in determining the structure of H_3^+ , with early efforts suggesting it was linear, and the final paper in the series (Hirschfelder 1938) concluding that the equilibrium structure 'lies between the right and equilateral triangular configuration'.

These difficulties in determining the minimum energy structure of H_3^+ are actually not surprising as the potential energy surface for the ion is now known to be rather flat. With the advent of electronic computers, accurate *ab initio* electronic-structure calculations became feasible. The first of these on H_3^+ (Christoffersen 1964) showed that the equilibrium structure of the ion was, in fact, an equilateral triangle. A result only confirmed experimentally sometime later (Gaillard *et al* 1978) using a Coulomb explosion technique.

At equilibrium the three hydrogen atoms are separated by $1.65a_0$ (0.873 \AA). Each proton thus shares equally the two electrons available to the system. This somewhat unconventional bonding structure is unknown in other hydrogenic systems but bears some similarities to the usually accepted structure of benzene where some of the bonding electrons are considered to be delocalized across the six carbon atoms in the molecule. H_3^+ is bound by about 4.3 eV. Actually the experimental value of $4.37 \pm 0.02 \text{ eV}$ (Cosby and Helm 1988) is not quite consistent with theoretical estimates which are generally in accord with Lie and Frye (1992) who obtained 4.337 eV with a much smaller error of 0.002 eV. It is interesting to note that

similar disputes were in progress 30 years ago (Varney 1960, Christoffersen 1964); in that time the point of contention has moved from the second to the third significant figure of the binding energy.

The H_3^+ formation reaction (1.1) is exothermic by about 1.7 eV. In fact the proton affinity of H_2 is low compared to many other stable molecules (see Oka 1983). This means that while H_3^+ is a very stable species, it is also highly reactive. It acts as a strong protonating agent via the reaction



No electronic excited states of H_3^+ or indeed electronic spectrum of H_3^+ has been observed. The most extensive theoretical work on the excited electronic states of H_3^+ is by Schaad and Hicks (1974). They showed that the lowest excited state, which is $^3\Sigma_u^+$ state with a linear equilibrium geometry, has a minimum deep enough to support several vibrational levels.

H_3^+ dissociates to $\text{H}_2(^1\Sigma_g^+) + \text{H}^+$, but this dissociation limit only correlates with singlet states of H_3^+ . The next dissociation channel, $14\,625\text{ cm}^{-1}$ (1.81 eV) higher, is to $\text{H}_2(^2\Sigma_g^+) + \text{H}(^2\text{S})$. This channel can correlate with both singlet and triplet states of H_3^+ .

The $^3\Sigma_u^+$ state of H_3^+ lies above, but cannot access, the lowest-dissociation limit. It is thus expected to be metastable with a long lifetime. Alhrichs *et al* (1977) estimated the fundamental vibrational frequencies of the $^3\Sigma_u^+$ state using the harmonic approximation; Preiskorn *et al* (1991) performed a similar calculation using higher accuracy electronic wavefunctions. However, extensive calculations by Wormer and de Groot (1989) showed that the surface was too flat for the harmonic approximation to have any validity. In particular, the energy required to cross the barrier between linear structures with the atom ordering permuted is less than the zero-point energy predicted by the harmonic approximation. Under these circumstances the vibrational (and rotational) structure of the system is likely to have more in common with energy levels of a Van der Waals cluster than a rigidly bound system. It is possible that amongst the many H_3^+ lines that have been observed in hydrogen plasmas, some will belong to the $^3\Sigma_u^+$ state of H_3^+ . But in the absence of a full potential energy surface for this state and sophisticated ro-vibrational calculations, these transitions will remain among the many that have yet to be assigned.

The only electronically excited state for which there appears to be any experimental data is the first excited singlet state. This state also correlates with the $\text{H}_2(^2\Sigma_g^+) + \text{H}(^2\text{S})$ asymptote and its dissociation threshold was observed to be about 2.5 eV above that of the ground state by Bae and Cosby (1990), in general agreement with the calculations of Talbi and Saxon (1988).

2.3. Ground-state electronic-structure calculations

In the last 20 years the ground state of H_3^+ has been the subject of numerous electronic-structure calculations; a comparative tabulation of 43 such calculations can be found in Anderson (1992). Notable landmarks amongst these calculations are those by Carney and Porter (1974, 1976) which led to the first accurate and detailed predictions of the ro-vibration rational spectrum (see below). Meyer *et al* (1986) (usually called MBB) calculated a number of surfaces. The best of these has been used extensively for spectroscopic calculations and has proved to be of outstanding accuracy. In fact MBB's best surface is not fully *ab initio* in that they adjusted one parameter so that their surface reproduced the observed $\text{H}_3^+ \nu_2$ fundamental. The most accurate *ab initio* potential energy surfaces available are due to Lie and Frye (1992) and Röhse *et al* (1994). Recent calculations (Tennyson and Polyansky

1994, Dinelli *et al* 1995) have shown that, as far as reproducing the known spectroscopic data on H_3^+ is concerned, the largest error in this surface is due to the Born–Oppenheimer approximation. This will be discussed further below.

Ab initio calculations suggest that at about $14\,275\text{ cm}^{-1}$ (1.77 eV) above the equilateral triangle minimum H_3^+ can sample linear geometries. Above this energy the H atoms can thus freely interchange and the spectrum is subject to the sort of complications anticipated for the $^3\Sigma_u^+$ state of H_3^+ above. This energy regime is discussed in sections 11 and 12.

A number of calculations have concentrated on obtaining very accurate values for the electronic energy of H_3^+ in its equilibrium geometry. Amongst these are a series of quantum Monte Carlo calculations by Anderson. The most recent of these (Anderson 1992) predicted an H_3^+ energy of $-1.343\,835 \pm 0.000\,001 E_h$ †. This result is in exact agreement with the recent Hylleras CI result of Röhse *et al* (1993) who obtained an energy of $-1.343\,835\,1 E_h$ and estimated an error of less than $0.000\,001 E_h$. Unlike the other calculations discussed above, these calculations are not variational, i.e. they do not approach the true H_3^+ energy from above. However, it is interesting to use them to estimate the error in the earlier calculations: Hirschfelder (1938) was $11\,200\text{ cm}^{-1}$ above the true energy, Carney and Porter's (1974) calculation was 700 cm^{-1} too high, while MBB and Lie and Frye (1992) are only 164 and 9 cm^{-1} above the true Born–Oppenheimer limit for the system.

It should be noted that in the very precise calculations of Anderson (1992) and Röhse *et al* (1993) the dominant errors are not actually those quoted. The quoted errors are for the solution of the non-relativistic Schrödinger equation within the Born–Oppenheimer approximation. Estimates of the relativistic correction (Röhse *et al* 1993) and corrections to the Born–Oppenheimer approximation (Lie and Frye 1992) have been made but these quantities were not completely determined *ab initio*. Bardo and Wolfsberg (1978) used a self-consistent field (SCF) wavefunction to estimate the leading correction to the Born–Oppenheimer approximation, known either as the adiabatic or Born–Oppenheimer diagonal correction. Recently Dinelli *et al* (1994b) used a similar wavefunction but a much simpler treatment due to Handy *et al* (1986) to calculate this correction as a function of H_3^+ geometry, this will be discussed further in section 5.5.

All the calculations discussed above considered only the region about equilibrium which is important for spectroscopy. However, analysis of chemical reactions of the form



or the photodissociation spectrum of Carrington and co-workers requires global potential energy surfaces covering both the equilibrium structure and dissociation channels. Schinke *et al* (SDL) (1980) computed the only accurate *ab initio* global potential energy surface currently available. However, the SDL surface has a number of unsatisfactory aspects which means that after initial use for some quantal calculations (Tennyson and Sutcliffe 1984, 1985, Child 1986a, b, Pfeifer and Child 1987), it has not been widely used for calculations.

To construct a true global potential energy surface it is necessary to consider dissociation to both $H_2(^1\Sigma_g^+) + H^+$ and $H_2(^2\Sigma_g^+) + H(^2S)$. This is because for certain large H_2/H_2^+ bondlengths $H_2(^2\Sigma_g^+) + H(^2S)$ is actually the lower dissociation channel. Of course this also means that a full surface necessarily contains an avoided crossing.

One surface which has been widely used for studying the behaviour of H_3^+ at dissociation is the diatomics in molecules (DIM) surface of Preston and Tully (1971). This model actually gives surfaces for the lowest two 1A_1 states of H_3^+ by diagonalizing a 3×3 matrix at each

† $1 E_h = 27.21\text{ eV} = 2.194\,746 \times 10^5\text{ cm}^{-1}$.

geometry. These surfaces are qualitatively correct at all physically interesting configurations but are not particularly accurate. In particular the ground-state surface gives a much poorer representation than the *ab initio* potentials discussed previously of the low-lying energy levels of the system and overestimates the dissociation energy by about 2700 cm^{-1} (0.33 eV) (Miller and Tennyson 1988a).

Murrell *et al* (1984) in their book on molecular potential energy functions use H_3^+ as their example of a system which requires a multivalued surface to obtain a true representation of the global potential. They construct a global surface by solving a 2×2 matrix where the two dimensions correspond to surfaces which correlate with the two low-lying dissociation channels discussed above. As far as I am aware the H_3^+ surface they present, which, like the DIM potential, should be reliable for a large range of configurations, has never been used for quantitative work on H_3^+ . Perhaps surprisingly for such a simple and fundamental system, the question of an accurate, reliable and global surface for H_3^+ remains unresolved.

3. Importance of H_3^+ in the interstellar medium

3.1. Nature of the ISM

As we look into the night sky what we see is the many stars or even the centre of our galaxy, the Milky Way, shining at us. What we do not see are the vast cold molecular clouds which occupy the region between these stars, known by astronomers as the interstellar medium or ISM.

The growth of radio astronomy in the 1960s and 1970s led to the identification of many new and unexpected molecules in the ISM (see Lequeux and Roueff 1991 and Herzberg 1990a). Indeed there are some species which have yet to be observed in the laboratory, an example is the cyanacetylene family, HC_nN , where spectra have been observed for $n = 1, 3, 5, 7, 9, 11$ in the ISM (Winnewisser and Herbst 1993) but only $n \leq 9$ on Earth (Iida *et al* 1991). Radio astronomy is a very sensitive technique which detects molecules via their rotational spectrum. However, molecules which have no permanent dipole such as H_2 , H_3^+ or CH_4 cannot be observed in this fashion. Conversely molecules, such as the cyanoacetylenes mentioned above, can be seen in very low concentrations because they have a large dipole moment and, being linear, many transitions are coincident leading to a significant further increase in intensity.

The giant molecular clouds that exist in the ISM are very cold—temperatures in the range 10–100 K—and have densities which on earth would correspond to a very high vacuum—typical number densities are 10^4 – 10^6 particles per cm^3 . These conditions are not at all promising for a high level of chemical activity or diversity and initially astronomers were puzzled.

On Earth, a typical gas phase association reaction occurs between two neutral atoms/molecules with a (neutral) third body available to remove the excess energy. It is possible to form H_3^+ without the creation of intermediate H_2^+ via similar three-body reactions:



These reactions will occur in dense hydrogen plasmas. However, for the reactions to be significant, densities higher than those found in the upper atmospheres of the giant planets or standard laboratory experiments are probably required.

Neutral species often have an energy barrier to a reaction occurring at all; such reactions are characterized by reaction rates which increase rapidly with temperature. This model of chemical reactions is clearly inappropriate for the ISM where, at near vacuum pressures, three-body collisions are extremely unlikely and the low temperatures mean that any reaction barrier is likely to prove completely insurmountable. Alternative reaction schemes are clearly necessary.

One class of reactions responsible for seeding the various chemical pathways in the ISM are two-body ion-molecule reactions. These reactions are very rapid, often occurring at every collision, the so called Langevin rate, as they usually proceed without any barrier. Indeed the charge on the ion acts to polarize the molecule at long range leading to attraction between the species even at large distances. This can significantly enhanced collision cross sections which mean that these reactions can even proceed faster at low temperatures.

The major molecular species in the ISM is hydrogen and it is therefore not surprising that its most stable ionic form, H_3^+ , is the driving force behind the chain of ion-molecule reactions which result in the abundance of molecules observed. In a now classic paper, Herbst and Klemperer (1973) showed that H_3^+ was vital to the initiation of chemical processes in the ISM. This mechanism remains the accepted one despite the failure to detect H_3^+ in the ISM over the two intervening decades (see section 6).

3.2. Formation and destruction of H_3^+

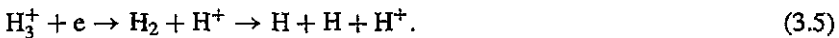
In the ISM, and elsewhere, the major formation mechanism of H_3^+ is via the reaction



Indeed, if, as is generally assumed, hydrogen is ionized in the ISM by cosmic rays, then one of the aims of trying to detect H_3^+ is to establish the flux of these rays (Dalgarno 1994). However, in hotter regions, such as shocked molecular clouds (see Flower 1989), where vibrationally excited molecular hydrogen is also present, it is possible to form H_2^+ and hence H_3^+ via



There are two major methods of removing H_3^+ from the ISM. One is through further chemical reactions, particularly protonation reactions (2.1); the other is via dissociative recombination:



The rate of destruction of H_3^+ via dissociative recombination (DR) is crucial for all aspects of the chemistry of the ISM. Radically different behaviour is displayed according to whether the rate is slow or fast (see for example Pineau des Forets *et al* 1992). However, DR rates are notoriously difficult to measure and to calculate. Several of them have been the subject of considerable controversy over the past decade. In this H_3^+ is something of a *cause célèbre*.

The generally accepted mechanism for DR, due to Bates (1950), is that the incoming electron attaches to the ion to form a long-lived state (resonance) which then dissociates via a curve crossing between the neutral resonance state and the ion. However, for H_3^+ at low energy, no such curve crossings have been found and early theoretical calculations suggested that the DR was indeed slow (Kulander and Guest 1979, Michels and Hobbs 1984). In contrast, a number of experimental studies during the same period suggested a

fast DR rate in the range $1-2 \times 10^{-7} \text{ cm}^3 \text{ s}^{-1}$ (see Macdonald *et al* 1984 and references therein).

However, in the mid-1980s Adams and Smith (1987, 1988) performed a series of measurements that suggested that the rate could be as low as $10^{-11} \text{ cm}^3 \text{ s}^{-1}$. They argued, persuasively given the history of other DR measurements, that the higher rates were due to contamination by vibrationally hot ions which have DR cross sections many orders of magnitude higher than the ground state. Amano (1988, 1990) subsequently performed spectroscopically based measurements which measured DR from the vibrational ground state directly. He obtained a rate coefficient of $1.8 \times 10^{-7} \text{ cm}^3 \text{ s}^{-1}$ at room temperature. The interpretation of his data was subsequently questioned (Adams and Smith 1989).

Recently there have been a number of measurements using differing experimental techniques (Canosa *et al* 1992, Larsson *et al* 1993, Smith and Spanel 1993, Sundstrom *et al* 1994) which all broadly agree with Amano's result (the spread is still about one order of magnitude). Bates (1993) proposed a theory which can give fast DR even in the absence of curve crossings; however this theory remains only qualitative. For the isoelectronic system HeH^+ , which also has no curve crossings at low collision energies, recent calculations have predicted large DR cross sections (Guberman 1994, Sarpal *et al* 1994). The mechanism for DR is provided by tunnelling at the inner turning point of the potential energy curve. However, for HeH^+ the experimental evidence on the DR rate is also controversial.

All-in-all the fast DR rate of H_3^+ is now generally accepted (Bates *et al* 1993). Even so there is still some way to go until 'experiment and theory (are) reconciled', as claimed by Smith and Spanel (1993) in the title of their paper.

In the interstellar medium H_3^+ acts as a vigorous protonating agent. For example H_3^+ protonates the otherwise chemically inactive CO molecule:



and the presence HCO^+ is often taken to correlate with that of H_3^+ . Figure 1 illustrates the role of H_3^+ in reactions in the ISM involving oxygen bearing molecules. H_3^+ is similarly important for nitrogen containing molecules, for example protonating HCN to give HCNH^+ , but is less important for reactions involving carbon species. Figure 1 is actually based on one given by Van Dishoeck (1986) which contains a detailed discussion of the chemistry of the ISM.

3.3. H_2D^+ and deuterium fractionation

The cosmic abundance of deuterium is generally accepted to be about 10^{-5} of that of hydrogen. Yet some molecules, such as DCO^+ , have been observed in cold molecular clouds with abundances approaching those of their normal hydrogen isotopomers. The process which leads to enhanced deuterium abundances is known as deuterium fractionation and it is one in which H_3^+ and H_2D^+ play a major role.

The driving force behind deuterium fractionation is that all molecules, even at absolute zero, retain some zero-point vibrational motion. This zero-point energy is inversely proportional to the square root of the reduced mass of the molecule. Thus heavier isotopomers (such as H_2D^+ compared to H_3^+) will be slightly lower in energy. This means that reactions such as



are slightly exothermic; in this case by 509 K (0.04 eV).

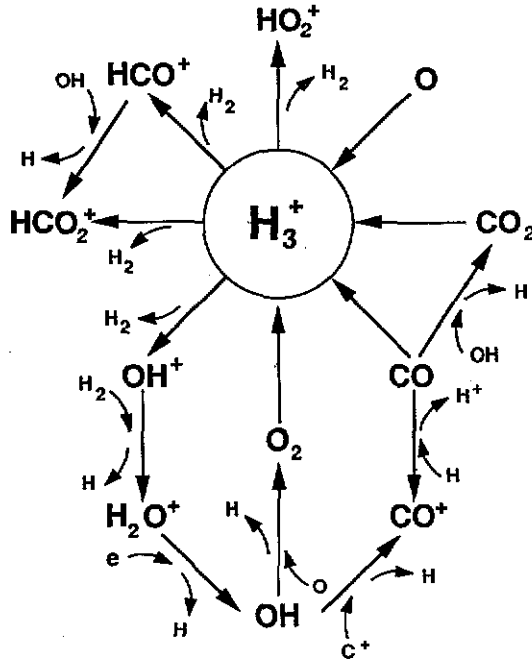


Figure 1. The most important chemical reactions in diffuse interstellar clouds involving oxygen-bearing molecules. This figure has been redrawn from Van Dishoeck (1986) to emphasize the importance of H_3^+ and is reproduced, with permission, from Miller and Tennyson (1992).

The major form of hydrogen in the ISM is not atomic but molecular. This means that deuterium fractionation involving HD is actually dominant:



In this case it is necessary to consider the difference between zero-point energies of H_3^+ and HD and those of H_2D^+ and H_2 . Because H_3^+ has three vibrational degrees of freedom against H_2 's one, this still yields an exothermic reaction. However, in the case of H_3^+ there is a second source of energy in this reaction. This is because, for reasons discussed in section 4.4, the $J = 0$ rotational ground state of H_3^+ cannot be populated but that of H_2D^+ is. As the lowest $J = 1$ state of H_3^+ is 64 cm^{-1} above the notional $J = 0$ state, this yields a further 92 K of energy. The net result is that this reaction is exothermic by 139.5 K.

This degree of exothermicity will not significantly alter the balance between H_3^+ and H_2D^+ at room temperature, but at temperatures of 10–20 K models show H_2D^+ number densities approaching those of H_3^+ . For a detailed discussion of deuterium fractionation effects see Brown and Rice (1986) and Millar *et al* (1989). Sidhu *et al* (1992) obtained very accurate estimates for the temperature-dependent equilibrium constants for reactions (3.7) and (3.8) using partition functions obtained from *ab initio* energy levels. Sidhu *et al*'s equilibrium constant for the dominant reaction, (3.8), is consistent with the ratio of the forward reaction rate extrapolated from high-temperature measurements by Smith *et al* (1982) and the reverse rate estimated theoretically by Herbst (1982). Recently, however, Gerlich (1993) has suggested that the forward reaction rate is almost five times slower than suggested. If this is true, then considerable revision of the deuterium fractionation models will be required.

4. Spectroscopy

4.1. Symmetry

As the equilibrium geometry of H_3^+ is an equilateral triangle it has high symmetry. This has a number of consequences for its spectroscopy which makes it unusual if not unique. The most obvious consequence, as the symmetry of the equilibrium geometry means that the ion has no permanent dipole moment, is that H_3^+ has no pure rotational spectrum.

In fact phenomenological (Pan and Oka 1986) and *ab initio* (Miller and Tennyson 1988b) calculations predict that H_3^+ should have an observable 'forbidden' rotational spectrum. This is because as the molecule rotates, it also distorts slightly about its rotation axis. Any distortion which leads to the three H atoms becoming inequivalent will result in the temporary formation of a dipole moment which can drive rotational transitions. Not surprisingly, as the degree of distortion rises rapidly with rotational quantum number, the predicted strength of these transitions rises very rapidly with the degree of rotational excitation. If J is the rotational angular momentum, then the intensity scales approximately as J^4 . Although this spectrum has yet to be seen, other 'forbidden' H_3^+ transitions have been observed (see below) and the predicted intensities for the pure rotational transitions are well within the capabilities of current technology.

As a non-linear triatomic molecule, H_3^+ possess three vibrational modes. However, the use of either the D_{3h} point group symmetry or the isomorphic complete nuclear permutation inversion symmetry $S_3 \times E^*$ (Bunker 1979) shows that there are only two unique vibrational motions. One mode is the totally symmetric (A_1') 'breathing' mode in which the molecule expands and contracts as an equilateral triangle. This mode is conventionally labelled ν_1 . The other is a doubly degenerate (E') bending mode, ν_2 . As degenerate vibrational modes also carry angular momentum, bending states are labelled ν_2^ℓ , where ν_2 is the number of quanta of vibrational excitation in ν_2 and the ℓ quantum number represents the vibrational angular momentum. Allowed values of ℓ range from $-\nu_2$ to $+\nu_2$ in steps of two. Vibrational states for which ℓ is not divisible by 3 are two-fold degenerate and thus have E' symmetry. States with $\ell = 0$ are non-degenerate and have A_1' symmetry. States with $\ell = 3, 6, \dots$ are split into A_1' and A_2' pairs.

As might be expected for a high symmetry system, there are rigorous, symmetry dictated, selection rules for dipole allowed transitions between different rotation-vibration levels of the system. Clearly the breathing mode, like the vibrational ground state, has no dipole moment. As the dipole does not change upon breathing excitation, pure breathing transitions are forbidden. Conversely, the bending mode does have a dipole (the H_3^+ dipole also has E' symmetry) and excitation of the bending mode is thus allowed. In general $A \leftrightarrow E$ and $E \leftrightarrow E$ transitions are symmetry allowed.

If the H_3^+ potential is considered as a harmonic, then more severe selection rules follow. In the harmonic model only excitation of the bending mode by a single quantum ($\Delta\nu_2 = 1$) is allowed and the associated ℓ quantum number also only changes by one. In practice H_3^+ is a rather floppy system which does not behave as a set of harmonic oscillators. This means that the harmonic selection rules are poorly observed, with significant consequences as discussed below. However, the transitions of H_3^+ do show a propensity for changes in ℓ to be small.

4.2. Vibration-rotation energy levels

Figure 2 shows the vibrational levels of H_3^+ calculated by Miller and Tennyson (1987) using the *ab initio* potential of Meyer *et al* (1986). Depicted on this figure are all the vibrational

bands which have so far been observed. The figure is drawn so that vertical transitions should be forbidden as they represent a change only in the ν_1 breathing mode and allowed transitions should involve a diagonal shift by one place to either the left or right. As can be seen, some of the transitions that have been observed are indeed forbidden. All the bands that have been observed in the laboratory will be discussed in the next section.

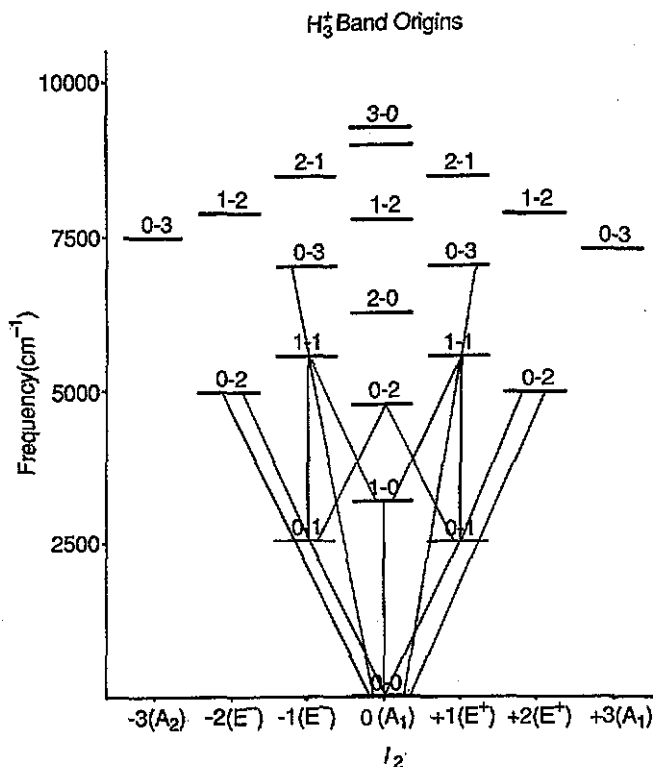


Figure 2. Band origins for H_3^+ computed by Miller and Tennyson (1987) using the MBB potential (Meyer *et al* 1986). Vibrational bands for which transitions have been observed are indicated (see table 1). The individual levels have been labelled by vibrational quantum number (ν_1, ν_2) and the levels are stacked according to the vibrational angular momentum quantum number ℓ . States with $\ell = \pm 1$ or ± 2 are degenerate. 'Allowed' transitions have $\Delta\ell = 1$.

Vibrational transitions do not occur in isolation. Associated with the change in vibrational quantum numbers there are changes in rotational quantum numbers. Because of the high symmetry and the vibrational angular momentum associated with X_3 molecules, the exact structure of the ro-vibrational levels of H_3^+ is complicated even in the low-energy region where a near harmonic model is still appropriate.

For a symmetric top molecule such as H_3^+ , the projection of the rotational angular momentum, J , along the symmetry axis of the top is conventionally designated K . K is usually considered a good quantum number. However, one has also to allow for the vibrational angular momentum. The quantum number ℓ discussed above is also a projection along the same axis. The conserved quantity is in fact $|K - \ell|$ which is often denoted G (Watson 1984). Furthermore, for vibrational states with non-zero ℓ a further quantum number, U , is required. These quantum numbers have been used to label the transitions

Table 1. Summary of the observed infrared transitions of H_3^+ and its deuterated isotopomers. The references are to the first observation of each band.

Transition	Reference
H_3^+	
$\nu_2(\ell = 1) \leftarrow 0$	Oka (1980)
$\nu_1 \leftarrow 0$	Xu <i>et al</i> (1992)
$2\nu_2(\ell = 2) \rightarrow 0$	Majewski <i>et al</i> (1989)
$2\nu_2(\ell = 0, 2) \leftarrow \nu_2(\ell = 1)$	Bawendi <i>et al</i> (1990)
$\nu_1 + \nu_2(\ell = 1) \leftarrow \nu_2(\ell = 1)$	Xu <i>et al</i> (1992)
$\nu_1 + \nu_2(\ell = 1) \leftarrow \nu_1$	Bawendi <i>et al</i> (1990)
$3\nu_2(\ell = 1) \leftarrow 0$	Lee <i>et al</i> (1991)
H_2D^+	
$\nu_1 \leftarrow 0$	Amano and Watson (1984)
$\nu_2 \leftarrow 0$	Foster <i>et al</i> (1986a)
$\nu_3 \leftarrow 0$	Foster <i>et al</i> (1986a)
D_2H^+	
$\nu_1 \leftarrow 0$	Lubic and Amano (1984)
$\nu_2 \leftarrow 0$	Foster <i>et al</i> (1986b)
$\nu_3 \leftarrow 0$	Foster <i>et al</i> (1986b)
D_3^+	
$\nu_2(\ell = 1) \leftarrow 0$	Shy <i>et al</i> (1980)
$2\nu_2(\ell = 2) \leftarrow 0$	Amano <i>et al</i> (1994)
$2\nu_2(\ell = 0, 2) \rightarrow \nu_2(\ell = 1)$	Amano <i>et al</i> (1994)
$\nu_1 + \nu_2(\ell = 1) \rightarrow \nu_2(\ell = 1)$	Amano <i>et al</i> (1994)

given in table 2 later. A thorough analysis of this problem has been given by Watson (1984) but is beyond the scope of this review.

There are rigorous rotational selection rules which accompany vibrational transitions. Parity considerations show that for H_3^+ ΔK must be odd (Oka 1992b). For any molecule, the properties of a dipole under rotation means that for a dipole transition the rotational quantum number, J , can change by only -1 , 0 and $+1$. In many molecules these transitions give rise to well defined regions of the vibrational band known as P, Q and R branches respectively. Recognizing these features, which often comprise series of regularly spaced transitions, and associated properties, for example Q branches are absent in certain classes of transitions, provide important pointers to which transitions are being observed. This analysis which leads to labelling the states involved in a transition with vibrational and rotational quantum numbers is usually called assignment.

The rotation-vibration spectrum of H_3^+ does not divide neatly into identifiable and regularly spaced P, Q and R branches. Because H_3^+ is so light, the rotational constants which determine the spacing of the rotational levels are very much larger than typical molecules. This combined with unusual selection rules means that the spectra of H_3^+ are highly irregular (see figure 3 for example). An extreme illustration of this was the first ever extra-terrestrial recording of an H_3^+ spectrum by Trafton *et al* (1989b). These workers originally thought they had recorded the spectrum of at least three different molecules! This spectrum, which is discussed in detail below, was only understood by Drossart *et al* (1989) by reference to detailed and accurate *ab initio* calculation.

4.3. Deuterated species

Often isotopic substitution only slightly modifies the spectrum of a molecule. Again H_3^+ is

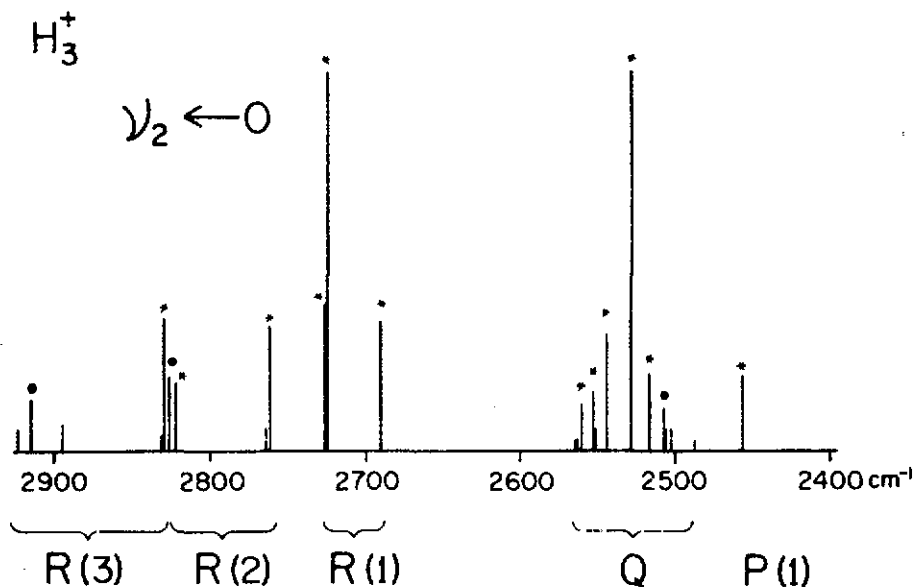


Figure 3. Stick representation of the observed *infrared* of the ν_2 fundamental spectrum of H_3^+ . The spectrum was obtained by Oka (see Oka 1983) in a liquid nitrogen discharge which gives H_3^+ with an effective rotational temperature of about 200 K.

an exception to this rule. The partially deuterated ions H_2D^+ and D_2H^+ have very different spectra to H_3^+ due to their lower symmetry. Both have allowed pure rotational spectra caused by the fact that the centre of mass and centre of charge no longer coincide. The resulting dipole moments are strong enough to generate an easily measured spectrum.

In H_2D^+ and D_2H^+ the degenerate ν_2 bending mode of H_3^+ (and D_3^+) is split by the lower symmetry into a bending mode and an antisymmetric stretch, conventionally labelled ν_2 and ν_3 respectively. These modes are well separated but are strongly coupled by Coriolis forces. All the three vibrational fundamentals of H_2D^+ and D_2H^+ have dipole allowed transitions and have been observed (see table 1).

4.4. Nuclear spin effects

The ground electronic state of H_3^+ is totally symmetric but the H atom has a nuclear spin of a half and is thus a fermion. The three nuclear spins in H_3^+ can couple to a total spin state of three halves, which has symmetry A_2 and fourfold degeneracy, or one half, which has symmetry E and a degeneracy of two. As in the well known H_2 case, these states are labelled ortho (for orthodox or more common) and para (for paradox or rarer) respectively. The Pauli principle means that rotation-vibration states with A_1 symmetry can never be populated; a fact which has not stopped most theoretical studies on H_3^+ calculating the energies of these states.

It should be stressed that the Pauli principle applies to the entire wavefunction of the system. This means that vibrational states, including the ground state, which have A_1 symmetry can still be populated *provided* the corresponding rotational state does not have the totally symmetric A_1 state. One consequence of this is that the $J = 0$ state of the vibrational ground state, which under other circumstances would be the ground state of H_3^+ , does not exist and the lowest level of the system has $J = 1$.

As the deuteron is a spin-one boson, nuclear spin statistics affect D_3^+ differently. In particular all symmetries of D_3^+ are allowed. H_2D^+ and D_2H^+ are somewhat simpler and form ortho/para states in a similar fashion to H_2 and D_2 respectively.

5. Laboratory spectra of H_3^+

5.1. The first detection

The search for a spectrum of H_3^+ was a long one with a number of false dawns. In particular initial attempts to observe and claims to have observed an optical spectrum of H_3^+ all came to nothing (see Oka 1983). Instead Herzberg (1967) embarked on a campaign to observe the ν_2 fundamental of H_3^+ in the *infrared*. He did not actually succeed in this attempt but instead happened upon a rich spectrum due to H_3 (and D_3 , see Herzberg 1987, 1990b).

The ground electronic state of H_3 is usually described as dissociative. In practice, it has a very shallow Van der Waals minimum which supports only a very few bound states (Tennyson 1982). However, all ions, both atomic and molecular, support infinite series of diffuse states where an extra electron is held in an orbital which look increasingly hydrogen-atom like as the excitation energy of the state increases. These are called Rydberg states and it transpires that the H_3 $2p\ ^2A_2''$ Rydberg state is very long lived (Lembo *et al* 1989) and amenable to spectroscopy (Figger *et al* 1989, Ketterle *et al* 1989b). In fact it was from studying transitions involving this state that the first, indirect, measurement of the totally symmetric ν_1 breathing fundamental of H_3^+ was made by Ketterle *et al* (1989a); but this is jumping ahead.

As already mentioned, Carney and Porter (1974, 1976) made detailed *ab initio* predictions of the spectrum of H_3^+ . Besides line positions, they also estimated the intensity of the ν_2 fundamental band. This, combined with technological advances in long column glow discharges and tunable laser *infrared* sources, persuaded Oka (see Oka 1983) to search for this band. After nearly five years of trying he eventually identified 15 lines in ν_2 fundamental band (Oka 1980) which were rapidly assigned by Watson using programs he developed to assign the H_3 Rydberg spectra discussed above. The *ab initio* predictions of Carney and Porter (1980) were accurate to about 7 cm^{-1} , an error of about 0.3%, for D_3^+ and were marginally worse for H_3^+ .

Figure 3 shows an idealized version of the ν_2 spectrum recorded by Oka. The lines are labelled according to whether they belong to the P, Q or R branches discussed above (the numbers in brackets correspond to the rotational quantum number of the lower level). What is noteworthy about the spectrum is the gap of more than 100 cm^{-1} between the Q branch and the R(1) transitions. This gap is a consequence of the absence of $J = 0$ state of the vibrational ground state caused by the Pauli principle. This gap thus confirms that the spectrum is of a molecule containing three identical fermions.

As it turned out, only a matter of weeks after Oka's detection, Shy *et al* (1980) recorded eight lines from the D_3^+ ν_2 fundamental using a completely different experimental technique. Four of these lines were assigned using Carney and Porter's calculations, but a full assignment of the spectrum had to await a more extensive treatment by Watson *et al* (1987).

5.2. Variational calculations

Traditionally molecules are thought of as near-rigid bodies which undergo only small amplitude motion about some (equilibrium) geometry. This view leads to a model of

molecular rotations based on the rotations of a rigid body and vibrations based on the harmonic approximation. Within this model, *ab initio* predictions of rotation–vibration spectra are fairly straightforward and rely solely on the ability to solve the electronic-structure problem for the molecule in question. The rotational structure is then determined by the predicted equilibrium structure and the (harmonic) vibrational frequencies are obtained from second derivatives of the potential at this point.

Of course it has long been accepted that the rigid-rotor harmonic oscillator model of molecular spectra is not fully quantitative. As a result sophisticated perturbation expansions based on these models have been derived and successfully applied to many systems. Indeed the rotational constants and force constants, which are the result of such perturbation theory analysis, are the common currency of most of high-resolution spectroscopy.

However, molecules which undergo large amplitude vibrational motions are not natural candidates for a rigid-rotor treatment. It is well known (Carney *et al* 1978) that molecules containing hydrogen are particularly anharmonic. Thus H_3^+ , containing only H atoms, can be expected to be particularly poorly behaved.

Since the mid-1970s a number of more exact methods for calculating molecular spectra have been developed. They are often collectively described as variational methods as they use computational procedures based upon the variational principle (see McWeeny 1989) to solve the nuclear motion problem. These methods generally attempt to calculate energy levels and wavefunctions for the exact problem making only the Born–Oppenheimer approximation. Tennyson and Miller (1992) give a simple introduction to these calculations; the scope of which are discussed by Tennyson (1992).

Molecules are composed of both electrons and nuclei, both of which move. However, the electrons are nearly 2000 times lighter than the lightest nucleus (that of hydrogen) and therefore move much more quickly. The Born–Oppenheimer approximation assumes that the electrons relax instantly to any change in nuclear geometry. This means that electronic-structure and nuclear-motion problems can be tackled separately. Within the Born–Oppenheimer approximation, the potential energy surface, which is the sum of the electronic energy and the nuclear repulsion energy as a function of internuclear coordinates, forms the link between the electronic and nuclear motion problems. For triatomic molecules such as H_3^+ the potential function is a three-dimensional (3D) hypersurface. Within the Born–Oppenheimer approximation the same potential energy surface is appropriate for H_3^+ , H_2D^+ , D_2H^+ and D_3^+ .

The strategy for calculating spectra from first principles is then as follows. First it is necessary to compute the electronic potential at a grid of geometries. These computed energies are then usually fitted to some functional form to give a prediction for the potential at all the geometries of interest. The motions of the nuclei on this potential are then represented using basis functions to give a secular matrix which is then diagonalized to give the rotation–vibration energy levels. It is just such a procedure which Carney and Porter (1974, 1976, 1980) used for H_3^+ and which has been used by many workers since.

In fact Carney and Porter worked in so-called Eckart coordinates (see Carney *et al* 1978). These are body-fixed coordinates which are related to normal coordinates of vibration and are obtained by using the Eckart conditions to obtain an optimal separation of vibrational and rotational motion (Sutcliffe 1980). There are technical problems with Eckart coordinates which means that most work on H_3^+ subsequent to Carney and Porter has used internal coordinates. These coordinates, for which Hamiltonians have to be derived in each case (Sutcliffe 1982), are defined in terms of geometric parameters giving the relative position of the nuclei in the molecule, see Sutcliffe and Tennyson (1991) for a rather general example.

Much of the theoretical work on H_3^+ and its isotopomers, including all that I have been

involved in, has been based on scattering (or Jacobi) coordinates, see figure 4. In fact these coordinates, which have a number of computational advantages (Tennyson 1986, Tennyson *et al* 1992), do not carry the full symmetry of the H_3^+ system and are therefore less than ideal.

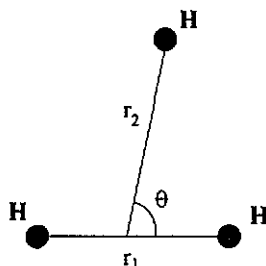


Figure 4. Scattering or Jacobi coordinates used for many variational calculations on H_3^+ . Note that these coordinates do not possess the full symmetry of the system.

There are a number of coordinates which carry the full (vibrational) symmetry of H_3^+ . Calculations on H_3^+ have been performed using symmetrized scattering coordinates by Day and Truhlar (1991) and Bačić and Zhang (1991, 1992), but such calculations entail the use of non-orthogonal basis sets. Calculations have also been performed in hyperspherical coordinates (Bartlett and Howard 1990, Whitnell and Light 1989, Carter and Meyer 1990, 1994, Wolniewicz and Hinze 1994) and most recently in perimetric coordinates (Sutcliffe 1992, Wei and Carrington 1994). All these symmetrized coordinates systems are considerably more elegant than the scattering coordinates of figure 4, but technically more difficult. As yet none has been used for detailed spectroscopic analysis of H_3^+ . Finally mention should be made of Jensen and co-workers (Špirko *et al* 1985, Jensen *et al* 1986, Jensen and Špirko 1986) who used atom-atom coordinates for treating the H_3^+ and related problems. Similar coordinates have also recently been used by Watson (1994).

Besides changes in coordinate systems, the main advances since the work of Carney and Porter include the calculation of more accurate potential functions, discussed above, the use of two-step variational procedures for treating rotational excitation and the emergence of finite element techniques, particularly the discrete variable representation (DVR), for treating high levels of vibration excitation. This last will be discussed in section 12.2.

The two-step procedure for rotational motion, which was proposed independently and in a slightly different form by Chen *et al* (1985) and Tennyson and Sutcliffe (1986), relies on performing one or more vibrational calculation and using the solution of this to treat the fully coupled rotation-vibration problem. Chen *et al* used solutions of the rotationless, $J = 0$, problem as a basis for the full rotation-vibration problem, while Tennyson and Sutcliffe used a series of $J + 1$ calculations for each state with rotational quantum number J . Each of these calculations were for a different value of $|k|$, the projection k along the body-fixed z axis of the molecule. Clearly Chen *et al*'s method is cheaper for the vibrational step, but it is poor when molecules undergo significant rotational distortion and fails completely when molecules go from bent to linear geometries. Tennyson and Sutcliffe's method is more expensive but does not suffer from these problems. Both methods have been used by other workers, but Tennyson and Sutcliffe's method is better suited for a floppy system such as H_3^+ .

Prior to the introduction of the two-step procedure, variational calculations on all triatomic systems were restricted to calculations with $J \leq 4$. With this problem removed Miller and Tennyson (1988a) performed calculations to probe the rotational dissociation limit of H_3^+ and H_2D^+ , which they found to be at $J = 45$ and 54 respectively.

If actual spectra are required it is necessary to perform one more step in the calculation. It is necessary to construct a surface giving the dipole vector for each geometry; for H_3^+ only a two-dimensional (2D) dipole moment surface is required as the dipole is always zero in the direction normal to the plane of the molecule. Linestrengths are then obtained as the square of the transition dipole linking the states in question (see Jensen and Špirko 1986, Miller *et al* 1989 and Le Sueur *et al* 1993 for details of this procedure). It should be noted that this method of calculating transition intensities makes no assumptions about which transitions are allowed or forbidden and the only rigorous selection rules are those which come directly from angular momentum theory and other rigorous symmetry considerations. Furthermore one should note that as yet there have been no absolute intensities measured in *any* H_3^+ spectrum. This means that all information on linestrengths for individual transitions, which is of vital importance for all astronomical observations discussed below, comes from *ab initio* theory.

5.3. Fundamental, overtone and hot bands of H_3^+

Following the initial observation of the H_3^+ ν_2 fundamental by Oka (1980), the band has been analysed in some detail. This work (Watson *et al* 1984, Majewski *et al* 1987), in common with most of the high-resolution *infrared* spectroscopy of H_3^+ , was performed in Oka's group in Chicago and at the Herzberg Institute of Astrophysics in Ottawa, although some has been performed elsewhere (for example Nakanaga *et al* 1990). Very recently Oka's group (Uy *et al* 1994) have used a hot discharge to measure 72 transitions involving levels with rotational quantum number J as high as 16. Contrary to their initial expectations, and unlike carbocation plasmas, it transpired that the population of H_3^+ in these plasma is thermal.

Despite the assignment of many lines in the fundamental bands there remain many unassigned transitions in H_3^+ plasmas at all temperatures (for example see table VI in Xu *et al* 1992). Both the Chicago and Ottawa groups were studying these when the astronomical observation of H_3^+ at unexpected wavelengths (see section 7) gave a new urgency to these studies. In Ottawa, Majewski *et al* (1989) observed the H_3^+ $2\nu_2 \rightarrow 0$ overtone band in emission using a hot H_2 plasma, while in Chicago Bawendi *et al* (1990) observed transitions involving the same upper state via the $2\nu_2 \leftarrow \nu_2$ hot band. Assignment of both of these bands relied heavily on accurate theoretical predictions of line positions (Miller and Tennyson 1989). Bawendi *et al* (1990) also observed transitions from the hot band $\nu_1 + \nu_2 \leftarrow \nu_1$.

Lee *et al* (1991) managed to observe four lines in the second overtone band of H_3^+ , $3\nu_2 \leftarrow 0$. These transitions were observed despite being a factor of some 250 weaker than the fundamental (Dinelli *et al* 1992). Again they were assigned by reference to *ab initio* calculation. More recently Ventrudo *et al* (1994) have extended and corrected these observations. Assignment using the same *ab initio* calculations (Miller and Tennyson 1988c, 1989) showed that these calculations systematically underestimate the $3\nu_2$ band origin by approximately 3 cm^{-1} . This error is actually a reflection on the underlying potential (Meyer *et al* 1986) used for the calculations and is a problem which will be discussed further below. All the H_3^+ *infrared* transitions observed in the laboratory and space up to 1991, along with many *ab initio* predictions for transition frequencies and linestrengths, are compiled in Kao *et al* (1991).

The observation of overtone and hot bands in H_3^+ has meant that a detailed but partial picture was obtained in that several bending states of H_3^+ had been studied but, besides the $\nu_1 + \nu_2 \leftarrow \nu_1$ hot band, nothing was known about the stretching states. These states are important not only because of their obvious spectroscopic interest, but because they are likely to have long lifetimes. These metastable states are thus likely to exist for considerable periods in environments with few collisions. Such regimes exist both astrophysically and in most experiments to measure the DR cross section of ground-state H_3^+ , as discussed above.

The original experimental estimates of the ν_1 stretching frequency came from analysis of the analysis of H_3 Rydberg spectra (Ketterle *et al* 1989a, Lembo *et al* 1989), which proved to be in perfect agreement with the best available *ab initio* estimates (Miller and Tennyson 1988c). However, subsequently the Chicago group (Xu *et al* 1992) measured lines in both the ν_1 fundamental band and the $\nu_1 + \nu_2 \leftarrow \nu_2$ hot band. Although transitions in both these bands are formally forbidden, the mechanisms which allowed their observation actually differ. In the case of the ν_1 fundamental band, Xu *et al* were able to observe transitions to the ν_1 vibrational level with $J = 5, 6, 7$. For this range of rotational quantum numbers the ν_1 level overlaps the ν_2 level and the states become close enough for small mixing terms to be important. This mixing leads to the $\nu_1 \leftarrow 0$ transitions acquiring intensity; a process usually known as intensity stealing.

For the $\nu_1 + \nu_2 \leftarrow \nu_2$ band one should note that both vibrational states involved are of E symmetry. Although the transition is forbidden by the conventional harmonic oscillator selection rules, it is actually allowed by the $E \leftrightarrow E$ dipole selection rules based purely on symmetry and discussed above. Miller *et al* (1990a) calculated the intensity of this band and suggest that it should be observable. Figure 5, which is adapted from Xu *et al* (1992), shows typical examples of the observed forbidden transitions. For comparison with the observed transition frequencies, the *predicted* frequencies, calculated using first-principles quantum mechanics by Miller *et al* (1990a), are also shown. Clearly these predictions are excellent. Actually they are not only good, but too good as will be discussed further in section 5.5.

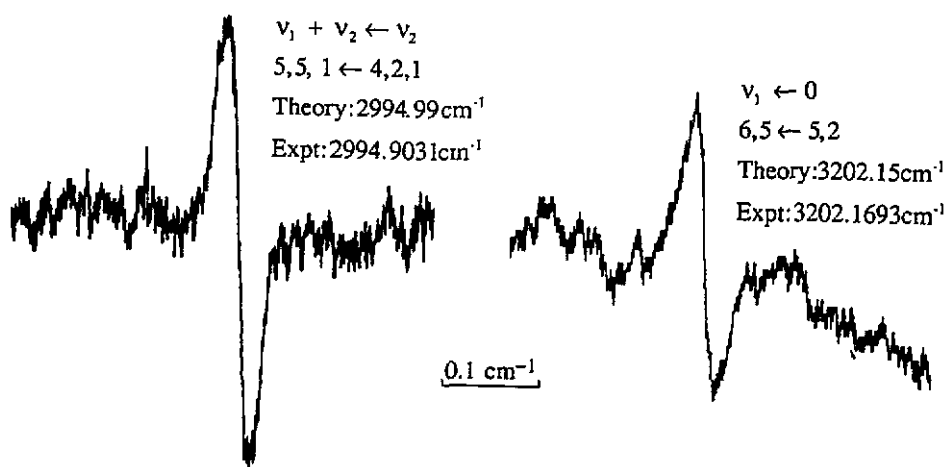


Figure 5. Typical examples of forbidden transitions observed by Xu *et al* (1992). The transition wavenumbers predicted by Miller *et al* (1990a) are given for comparison.

Steinmetzger *et al* (1982) obtained *infrared* emission spectrum tentatively assigned to H_3^+ , details of which can be found in Burton *et al* (1984). This spectrum was recorded from

the products of the H_3^+ formation reaction (1.1). However, the frequencies do not match the ones recorded above particularly well and it is unlikely that these emissions were due to transitions to ground-state H_3^+ .

Before leaving the topic of H_3^+ laboratory *infrared* spectra it is worth making a comment about band origins. Much of the early analysis of the H_3^+ spectra was performed using traditional spectroscopic techniques in terms of parametrized, effective Hamiltonians (Watson 1984). These Hamiltonians were later improved by using the Padé approximant representation of the effective Hamiltonian due to Polyansky (1985) but they still suffered from poor convergence which is an inevitable consequence of the lightness and strong Coriolis coupling found in H_3^+ . More recently analysis has been performed entirely in terms of matching observed frequencies with those obtained from first-principles calculations. This means that among the many parameters which are no longer determined experimentally is the vibrational band origin. Thus the band origins for the observed overtone and combination levels are only known from these calculations, perhaps with an empirically determined correction when some systematic error is observed.

5.4. Spectra of deuterated H_3^+

As mentioned above, the ν_2 fundamental of D_3^+ was observed by Shy *et al* (1980) almost simultaneously with Oka's detection of H_3^+ . A comprehensive study was performed by Watson *et al* (1987) who observed 60 lines in emission and, by combining them with previous data, fitted a total of 84 lines to an effective Hamiltonian. Recently Amano *et al* (1994) have returned to the D_3^+ problem and observed transitions in the $2\nu_2 \leftarrow 0$ overtone emission band as well as several hot bands. These transitions were assigned using a new variational calculation procedure developed for the purpose by Watson (1994).

The spectra of H_3^+ and D_3^+ can be analysed using similar procedures (Watson 1984, 1994). However, the spectroscopic behaviour of the mixed isotopomers, H_2D^+ and D_2H^+ , is fundamentally different. H_3^+ and D_3^+ are symmetric tops; H_2D^+ and D_2H^+ are (very) asymmetric tops. H_3^+ and D_3^+ have no permanent dipole moment and hence no observed rotational spectrum; H_2D^+ and D_2H^+ both have a sizeable permanent dipole, that of H_2D^+ in its ground state is 0.6055 D (Tennyson *et al* 1990b). Both molecules have rotational spectra. That of H_2D^+ has been extensively studied *ab initio* (Tennyson and Sutcliffe 1986, Miller *et al* 1989, Tennyson *et al* 1990b, Polyansky *et al* 1993), largely because of its complexity. This system is actually particularly interesting from the point of view of breakdown of the separation between rotation and vibration motion as the lightness of the system means that rotational and vibrational quanta are much closer than is usual. Furthermore H_2D^+ is a (very) asymmetric top which, especially in vibrationally excited states, has particularly strong Coriolis coupling.

There are no published laboratory observations of D_2H^+ rotational transitions and only two of H_2D^+ transitions. These are the $1_{10} \leftarrow 1_{11}$ transition at 12.4226 cm^{-1} , which was detected by Bogey *et al* (1984) and Warner *et al* (1984), and the $2_{20} \leftarrow 2_{21}$ at 5.20317 cm^{-1} discovered by Saito *et al* (1985). These lines were assigned using combinational differences from the *infrared* spectra (Amano and Watson 1984) discussed below and *ab initio* predictions (Carney 1980, Tennyson and Sutcliffe 1984). The lack of further laboratory work on this problem is surprising given the astronomical importance of H_2D^+ . In part the problem is that most of the lines in the H_2D^+ rotational spectrum lie in the far *infrared* which is a difficult region to work in. This problem has also impeded the observation of the 'forbidden' rotational spectrum of H_3^+ , discussed above, which lies in a similar spectral region.

In fact a single unpublished spectrum of Jennings *et al* (1990) contains as much experimental information as is available in the literature. These workers sought the $1_{10} \leftarrow 0_{00}$ of H_2D^+ . This line, although it lies at a difficult wavelength for observation, is by far the most promising for astronomical detection of H_2D^+ . Indeed a sighting has recently been claimed in Orion (Boreiko and Betz 1993). Jennings *et al* found this line at 1370146 MHz (45.703 cm^{-1}), very close to the value, 1370141 MHz, predicted by combinational differences from the *infrared* spectrum of Foster *et al* (1986a). In recording this spectrum Jennings *et al* observed a second, weaker transition nearby at 45.700 cm^{-1} . This they assigned to the D_2H^+ transition $2_{20} \leftarrow 2_{11}$ on the basis of *ab initio* estimates (Miller *et al* 1989). Jennings *et al* recorded a further D_2H^+ rotational transition, the $1_{11} \rightarrow 0_{00}$ line, at 45.254 cm^{-1} (see Polyansky and McKellar 1990). It is to be regretted that these observations have never been published.

The first spectrum recorded of a mixed isotopomer was by Shy *et al* (1981) who reported nine lines in the ν_2/ν_3 band of H_2D^+ . This vibrational assignment was based upon *ab initio* estimates of Carney and Porter (1977) but no rotational assignments were made. These observations were extended in a combined study by the Ottawa and Chicago groups (Foster *et al* 1986a) who assigned both spectra using effective Hamiltonians based on the Padé approximants of Polyansky (1985). These spectra are actually particularly difficult to interpret because the ν_2 and ν_3 band origins are very close together. The strong Coriolis coupling between rotational states associated with each of these levels means that the two vibrational bands become strongly coupled for $J > 4$ (Tennyson and Sutcliffe 1985).

Most of the other significant work on the *infrared* spectra of the mixed isotopomers has been performed in Ottawa. Foster *et al* (1986b) assigned 88 lines in the ν_2/ν_3 band of D_2H^+ . Amano and Watson (1984) recorded 27 lines in the absorption spectrum of the H_2D^+ ν_1 fundamental, with a further 10 lines observed later by Amano (1985). Lubic and Amano (1984) reported 35 lines in the equivalent spectrum of D_2H^+ . Assignments for these asymmetric systems are difficult and a number of reassignments have been necessary (Kozin *et al* 1988, Miller *et al* 1989, Polyansky and McKellar 1990).

5.5. Spectroscopically determined potential energy surfaces

It has long been recognized that spectroscopic data can be used to improve the underlying potentials. Carney and Porter (1980) reduced their errors by an order of magnitude by adjusting their equilibrium geometry and harmonic force constant. Despite the very high accuracy obtained in many of the subsequent variational calculations on H_3^+ and its isotopomers, there are still errors in the first-principles calculations.

For example the systematic 3 cm^{-1} underestimate of the $3\nu_2 \leftarrow 0\text{ H}_3^+$ second overtone transitions by Miller and Tennyson (1988c, 1989) has been noted by Ventrudo *et al* (1994). Miller and Tennyson's calculations were performed using the potential function of Meyer *et al* (1986) (MBB). Accurate as this potential is, it is still undoubtedly the main source of the error in these calculations.

In fact MBB present a number of potentials in their paper. The version which is generally used is a corrected seventh-order fit to the 87GTO calculation. In this potential one parameter, the force constant for the ν_2 mode, was adjusted so that the potential reproduced the observed H_3^+ ν_2 fundamental frequency as MBB noted that their potential was too soft in this coordinate. In making this adjustment, MBB performed variational calculations on H_3^+ which used the mass of an H atom for each of the nuclei in H_3^+ . Of course this gives a total mass of the system of three protons plus three electrons, or one electron too much. The error in the mass, 1 part in 5500, is similar in magnitude to the errors in many predictions from the MBB potential. However, using a more appropriate value for the mass of the system makes

these errors worse not better. Thus the highly successful series of calculations performed using the MBB surface are based on a slightly defective model which is hard to correct. Illustrative of this problem is the fact that calculations performed using the variationally much superior potential energy surface of Lie and Frye (1992) actually do not improve on predictions made with the MBB surface, and in some cases give worse results, particularly for the ν_1 modes (Tennyson and Polyansky 1994).

There is an alternative for a system, such as H_3^+ , where there is a wealth of spectroscopic data available. One can take an initial potential, such as that due to MBB, and systematically improve it. This is done by calculating transition frequencies, or other observed data, comparing the calculations with the measurements, adjusting the potential, recalculating and so on. This process, which is summarized in figure 6, continues until a satisfactory fit is obtained (or one's computer budget exhausted!).

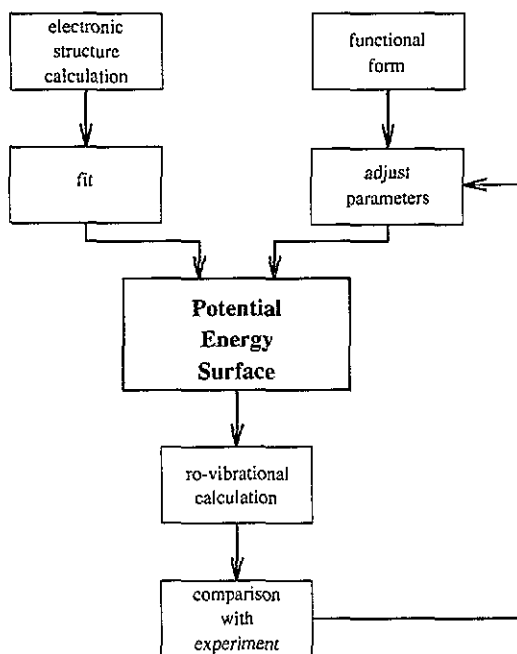


Figure 6. Schematic diagram of how potentials are produced *ab initio* (left-hand side) or by iterative fits to observed spectra (right-hand side).

This method has been used extensively for determining the potential energy surfaces of Van der Waals molecules (see Hutson 1990). Jensen and Špirko (1986) pioneered the use of such procedures for determining surfaces of chemically bound systems. Initial calculations were performed using programs specially developed to study H_3^+ and D_3^+ (Špirko *et al* 1985), and their mixed isotopomers (Jensen *et al* 1986). Preliminary calculations, presented in Jensen and Špirko (1986), gave a potential which reproduced 110 observed data points with a standard deviation of 2.2 cm^{-1} by adjusting nine parameters in the fit to the *ab initio* data points of Carney and Porter (1974).

However, this work coincided with the publication of the MBB potential (Meyer *et al* 1986). Calculations using this potential actually reproduced the laboratory data considerably

better than the fit of Jensen and Špirko. Indeed, as discussed above, predictions made using this potential were actually instrumental in assigning many of the H_3^+ hot bands and overtones. Jensen and Špirko therefore did not pursue their original goal of fitting H_3^+ but instead chose to study, with considerable success, systems which are less amenable to high accuracy *ab initio* calculation (see Jensen 1989 for example).

The next attempt to spectroscopically improve on the *ab initio* potentials was by Watson (1994). He developed a method for performing vibration-rotation calculations using Morse oscillators and internuclear distances which has strong similarities with the work of Jensen and Špirko (1986). The main difference being that Watson chose to use a DVR which allowed him to avoid some of Jensen and Špirko's approximations. He adjusted 7 of the 30 parameters in the MBB potential using 353 observed H_3^+ transitions (14 were omitted from the fit). The data used in the fit were reproduced with a standard deviation of 0.137 cm^{-1} . This procedure was then used to assign a number of new H_3^+ lines (Majewski *et al* 1994, Uy *et al* 1994) and was repeated for D_3^+ resulting in a number of new assignments, including for the $2\nu_2 \rightarrow 0$ overtone spectrum (Amano *et al* 1994).

Inspired by Watson's example, Dinelli *et al* (1994a) also decided to fit the H_3^+ data. They used 243 energy levels (rather than transitions) and tried starting from both the MBB potential and that of Lie and Frye (LF) (1992), which has the same functional form. They found that the LF potential gave the better starting point and by adjusting 11 parameters they reproduced the observed data with a standard deviation of 0.053 cm^{-1} . In fact further work and the reassignment of a few transitions has reduced this standard deviation by half (Polyansky *et al* 1995b).

Interestingly, tests on the deuterated species showed that the potential of Dinelli *et al* performed significantly worse for these species. In particular calculations on the mixed isotopomers H_2D^+ and D_2H^+ showed that the splitting between the ν_2 and ν_3 band origins could not be reproduced. Dinelli *et al* were forced to conclude this behaviour was associated with a break down of the Born-Oppenheimer approximation.

Tennyson and Polyansky (1994) used Dinelli *et al*'s effective H_3^+ potential along with fits to 89 transitions in the D_3^+ fundamental band to determine both the Born-Oppenheimer potential *and* the major mass-dependent correction to this potential, the so-called adiabatic or Born-Oppenheimer diagonal correction. These calculations showed that the major cause of error when predicting spectra using the LF potential, but not for MBB, is the Born-Oppenheimer approximation.

The adiabatic correction designed by Tennyson and Polyansky is only appropriate for the symmetric species, i.e. H_3^+ and D_3^+ . For the asymmetric isotopomers, H_2D^+ and D_2H^+ , the adiabatic correction also has an asymmetric, i.e. lower symmetry than D_{3h} , component. Polyansky *et al* (1995a) wrote the effective potential for each isotopomer as

$$V_{X_2Y^+}^{\text{eff}}(Q) = V^{\text{BO}}(Q) + \frac{1}{\mu_s(X_2Y^+)} \Delta V_{\text{sym}}^{\text{Ad}}(Q) + \frac{1}{\mu_a(X_2Y^+)} \Delta V_{\text{asym}}^{\text{Ad}}(Q) \quad (5.1)$$

with the mass (isotopomer) dependence given by the effective reduced masses

$$\frac{1}{\mu_s(X_2Y^+)} = \frac{2}{m_X} + \frac{1}{m_Y} \quad \frac{1}{\mu_a(X_2Y^+)} = \frac{1}{m_Y} - \frac{1}{m_X} \quad (5.2)$$

where m is the appropriate nuclear mass.

In (5.1), V^{BO} is the Born-Oppenheimer potential energy surface which can be determined by *ab initio* calculation or fitting; $\Delta V_{\text{sym}}^{\text{Ad}}$ is the symmetric contribution to adiabatic correction which has been determined *ab initio* by Dinelli *et al* (1995) or

spectroscopically by Tennyson and Polyansky (1994). $V_{\text{asym}}^{\text{Ad}}$ is the asymmetric contribution which only has C_{2v} symmetry and is important for determining the splitting between the ν_2 and ν_3 modes in H_2D^+ and D_2H^+ . There is insufficient experimental data available on the mixed isotopomers to determine this term fully. Polyansky *et al* (1995a) demonstrated that a form derived from the *ab initio* data of Dinelli *et al* (1995) removes the discrepancy in the splitting between the ν_2 and ν_3 band origins noted above.

6. Attempts to observe H_3^+ in the interstellar medium

6.1. Absorption spectra of H_3^+

The observation of H_3^+ in the laboratory by Oka (1980) led naturally to attempts to observe H_3^+ in the ISM. This is a difficult observation to attempt for a number of reasons. As the molecular regions of the ISM are very cold, H_3^+ will be found in very few levels. This completely rules out the possibility of seeing an emission spectrum, which requires H_3^+ at several hundred degrees Kelvin. In practice it is to be expected that only two levels of H_3^+ , with $(J, K) = (1, 1)$ and $(1, 0)$, will be found with a significant population. Remember that due to the Pauli principle, the $J = 0$ ground state of H_3^+ does not exist.

The ortho $(J, K) = (1, 0)$ state lies 22.84 cm^{-1} (33 K) higher than the para $(J, K) = (1, 1)$ ground state of the system. As in local thermodynamic equilibrium (LTE) the ortho state has twice the weight of the para state, LTE models suggest that the population of the two states should be comparable at typical ISM temperatures. There are a total six possible transitions, see table 2, involving these two rotational levels. All these lie in the $3.5\text{--}4.0 \mu\text{m}$ region known to astronomers as the L window. However, as it transpires, all these transitions lie near features in the Earth's atmosphere which complicate observations. This means, for example, that the exact Doppler shift between the target and Earth, which varies with the time of year, becomes a significant parameter. Furthermore, as the spectrum has to be recorded in absorption, it is necessary to have an *infrared* source on the far side of the object being observed. A number of attempts have been made to detect H_3^+ against the *infrared* continuum of various stars. Of these Oka (1981), Geballe and Oka (1989) and Black *et al* (1990) have actually published their results, see table 2. As yet no-one has managed to detect H_3^+ using this method.

Black *et al*'s observations are particularly interesting because they were able to obtain upper limits which begin to test theoretical predictions from models of the ISM. In particular their non-detection of H_3^+ only fits the models if cosmic-ray ionization rates are less than about 10^{-16} s^{-1} and their failure to observe H_3^+ in NGC2264 placed the tentative detection of H_2D^+ there (see below) in severe doubt. Although all the H_3^+ absorption studies to date have proved negative, there are many models which predict H_3^+ column densities $\sim 10^{14} \text{ cm}^{-2}$ (see Geballe and Oka 1989). Such column densities are just on the limits of the sensitivity of modern *infrared* spectrometers and, with improvements in technology and new spaceborne *infrared* spectrometers, it is hard to believe that the observation of H_3^+ in the ISM can long be delayed.

Recently Tennyson *et al* (1993) suggested that the assumption that the ratio of ortho- H_3^+ to para- H_3^+ in cold molecular clouds is thermal may be wrong. At the temperatures below 50 K thermal H_2 is almost entirely in its para form. In a series of papers Quack (1977, 1990) has argued on symmetry grounds that only para- H_3^+ can be formed from para- H_2 . Furthermore Quack suggests that conversion of para- H_3^+ into ortho- H_3^+ via proton hopping:



Table 2. H_3^+ ν_2 fundamental transitions potentially observable in absorption in the interstellar medium. Assignments, transition frequencies, Einstein A coefficients, A_{if} , and nuclear spin states from Kao *et al* (1991) are given for each transitions. Documented attempts to detect H_3^+ in the ISM using these features, all of which have proved negative, are also listed.

Line	$(J, K - \ell , U) \leftarrow (J, K)$	$\omega(\text{cm}^{-1})$	A_{if}/s	Spin
a	(2, 1, +1) \leftarrow (1, 1)	2726.219	60	Para
b	(2, 0, -1) \leftarrow (1, 0)	2725.898	99	Ortho
c	(2, 1, -1) \leftarrow (1, 1)	2691.444	52	Para
d	(1, 1, +1) \leftarrow (1, 1)	2545.418	66	Para
e	(1, 0, -1) \leftarrow (1, 0)	2529.724	129	Ortho
f	(0, 1, +1) \leftarrow (1, 1)	2457.290	119	Para

Reference	Lines	Objects observed
Oka (1981)	a, b	OMC-1 BN, IRC+10216, CIT, α Tau, α Lur, R Leo
Geballe and Oka (1989)	e f	GL2591, LkH α 101, OMC-1 BN, NGC2024, IRS2 W33 IR
Black <i>et al</i> (1990)	c	NGC2264 IRS, AFGL2591

will not occur in pure para H_2 . This reaction has always been assumed to be rapid (Black *et al* 1990). If Tennyson *et al*'s conjecture is correct, then attempts to detect H_3^+ in absorption should concentrate on using the two possible transitions of para H_3^+ . In fact most observations have used transitions of ortho H_3^+ , see table 2.

6.2. Attempts to detect H_2D^+ in the ISM

As discussed in section 3.3, deuterium fractionation can significantly raise the proportion of deuterated molecules, and in particular H_2D^+ , found in cold regions of the ISM. At 20 K, for example, fractionation can lead to $\text{H}_2\text{D}^+/\text{H}_3^+$ ratios of 0.05 compared to D/H ratio of 10^{-5} (Watson 1976).

Dalgarno *et al* (1973) suggested that H_2D^+ had a dipole strong enough for its rotational transitions to be observed in the ISM. However, attempts to detect H_2D^+ prior to the observation of laboratory spectrum all proved negative, see Angerhofer *et al* (1978) for example.

The main advantage of trying to observe H_2D^+ rather than H_3^+ is that it should be observable in emission. However, for H_2D^+ there is a trade-off between looking at very cold objects which should have a large H_2D^+ fraction, but in which the H_2D^+ will be largely in its rotational ground state, and warmer objects which will have proportionately less H_2D^+ but will show much more emission. The major problem with H_2D^+ observations is that, because the molecule is light, the transitions involving $J = 0$ and/or 1 lie at far infrared frequencies which are not observable from earth. However, the Kuiper Airborne Observatory has been used in the observations discussed below to provide a platform above the atmospheric water vapour.

Phillips *et al* (1985) looked for the $1_{11} \rightarrow 1_{10}$ line, which had just been observed in the laboratory, in the core regions of the molecular clouds NGC2264 and TMC-1. These targets were chosen on the basis of previous observations of DCO^+ . While the observations in TMC-1 were negative, they saw a weak feature in NGC2264 which they tentatively assigned to H_2D^+ . Subsequently attempts have been made by Pagini *et al* (1992a) and Van Dishoeck *et al* (1992) to observe this transition in a number of objects, including NGC2264, without success. The failure to observe anything despite large increases in sensitivity, about two

orders of magnitude in the case of Van Dishoeck *et al*, must cast considerable doubt on the original observation.

More recently Boreiko and Betz (1993) reported observation of the $H_2D^+ 1_{10} \rightarrow 0_{00}$ transition in the IRC2 region of the Orion Molecular Cloud (OMC-1). This transition is the most promising for astronomical observation as it involves the lowest two levels of H_2D^+ , and Boreiko and Betz's line is much stronger than any previous H_2D^+ features. However, Boreiko and Betz's models suggested that given their H_2D^+ observation, H_3^+ should be directly observable in absorption towards IRC2. Initial attempts to perform such an observation have failed to detect any H_3^+ (Geballe 1993) but the gas phase models of Pagini *et al* (1992b) emphasised the difficulty of deriving H_3^+ abundances from H_2D^+ observations.

7. H_3^+ in Jupiter

7.1. Detection

H_3^+ had long been an important component of Jovian ionospheric models (Atreya and Donahue 1976) and was detected *in situ* in the Jovian magnetosphere by the low-energy-charged-particle instrument carried by the Voyager spacecraft (Hamilton *et al* 1980, Krimigis and Roelof 1983). However, the real excitement over H_3^+ came with the serendipitous observation of an emission spectrum.

In September 1988, Drossart *et al* (1989) used the Canada-Hawaii-France Telescope to study the previously observed (Trafton *et al* 1989a, b) *infrared* emission spectrum of H_2 in the $2 \mu\text{m}$ region at high resolution. These emissions are *very* weak because H_2 has no dipole to drive these *infrared* vibration-rotation transitions. This means that the spectrum consists of quadrupole transitions which are very much less favoured. For example in the *infrared*, the dipole transitions of H_3^+ are up to 10^9 times as strong as the H_2 quadrupole transitions. The three hydrogen emission lines they sought were duly found (Kim *et al* 1990). However, in Jupiter's southern polar region, 33 further lines, some stronger than the H_2 transitions, were also observed. These unexpected lines were not observed on the body of the planet.

The new lines did not correspond to any published laboratory spectrum. Discussions with colleagues (see Oka 1992a) revealed that workers at the Herzberg Institute of Astrophysics in Ottawa had recorded a spectrum (later published as Majewski *et al* 1989) which showed some of the same features as those observed in Jupiter. At this stage it was not known whether this laboratory emission spectrum, which was obtained in a hot hydrogen discharge, was due to H_3^+ or Rydberg states of H_3 . Analysis by Watson, which used *ab initio* calculations (Miller and Tennyson 1989), data on the H_3^+ hot band $2\nu_2 \leftarrow \nu_2$ (later published as Bawendi *et al* 1990) and considerable electronic mail communication with Paris, London and Chicago showed that most of the unassigned lines were due the $H_3^+ 2\nu_2 \rightarrow 0$ emission band. Not all the H_3^+ Jovian emission features were observed in the laboratory spectrum, however detailed comparisons with the *ab initio* data showed that the transitions could be fitted by an H_3^+ rotational temperature of 1050 ± 100 K. Figure 7 compares the observations of Drossart *et al* (1989) with the *ab initio* calculation. After the assignment of this spectrum, it became apparent that it had actually been observed previously, but not assigned, by Trafton *et al* (1989b).

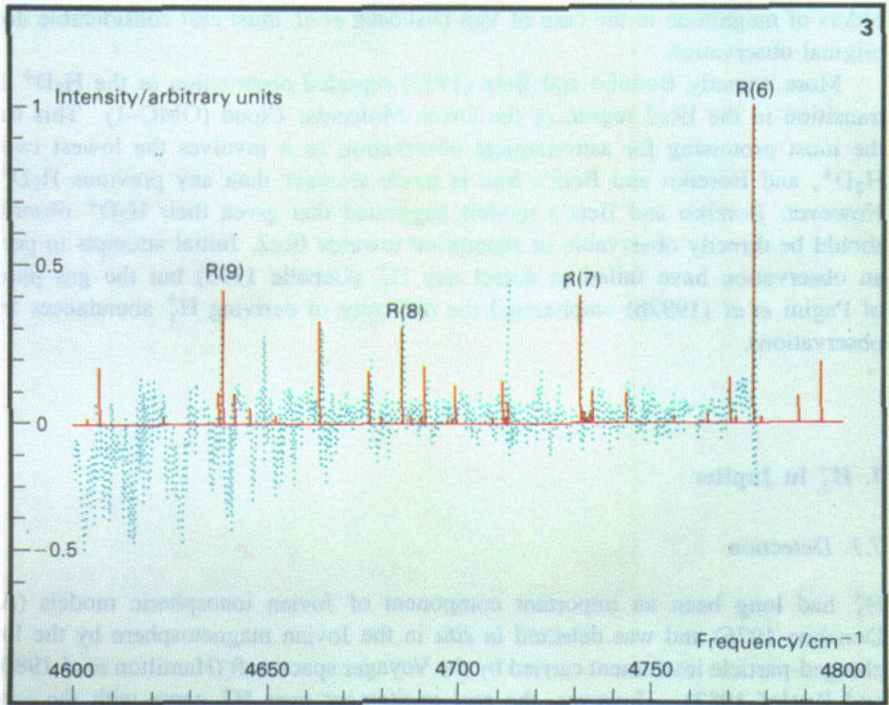


Figure 7. *Infrared spectrum of the south polar region of Jupiter as recorded by Drossart et al (1989) using the Canada–Hawaii–France Telescope. The blue line is the observed spectrum and the red sticks are *ab initio* predictions of the H_3^+ spectrum in this region, synthesized assuming an H_3^+ (rotational) temperature of 1000 K. The lines at 4713 cm^{-1} corresponds to the H_2 S(1) transition originally sought by Drossart and co-workers. The line at 4649 cm^{-1} remains unidentified. (Reproduced from *Chemistry in Britain* 26 1069 (1990).)*

7.2. Temperature of H_3^+ emissions

The surface of Jupiter is largely at temperatures of below 200 K. However, it has been known since the Voyager missions that Jupiter possessed hot regions in its poles. These had been studied both through the observation of a number of the *infrared* spectra of a number of unusual hydrocarbon species in the lower atmosphere and through the *ultraviolet* emissions of atomic and molecular hydrogen in the upper atmosphere (see Prangé 1991). Even so the rotational temperature of the H_3^+ emission detected on Jupiter at over 1000 K was surprisingly hot. A natural question immediately arose—was this rotational temperature a true thermal temperature or was the observed H_3^+ emission simply chemiluminescence following the formation of hot H_3^+ ?

The fundamental spectrum of H_3^+ , as observed by Oka (1980), has wavelengths in the region $3\text{--}5\ \mu\text{m}$. Luckily, much of this lies in a region of good atmospheric transmission, the so-called L window. Emission from the H_3^+ fundamental was originally observed by Oka and Geballe (1990) who interestingly failed to observe the corresponding $2\ \mu\text{m}$ spectrum and found that their H_3^+ had a temperature of only 670 K. Subsequent observations by Miller *et al* (1990b) and Maillard *et al* (1990) both suggested that vibrational temperatures and rotational temperatures were close to 1000 K, implying thermal equilibrium. This conclusion has recently been confirmed by Drossart *et al* (1993) using very high resolution Fourier transform *infrared* (FTIR) spectroscopy. These workers obtained line profiles for

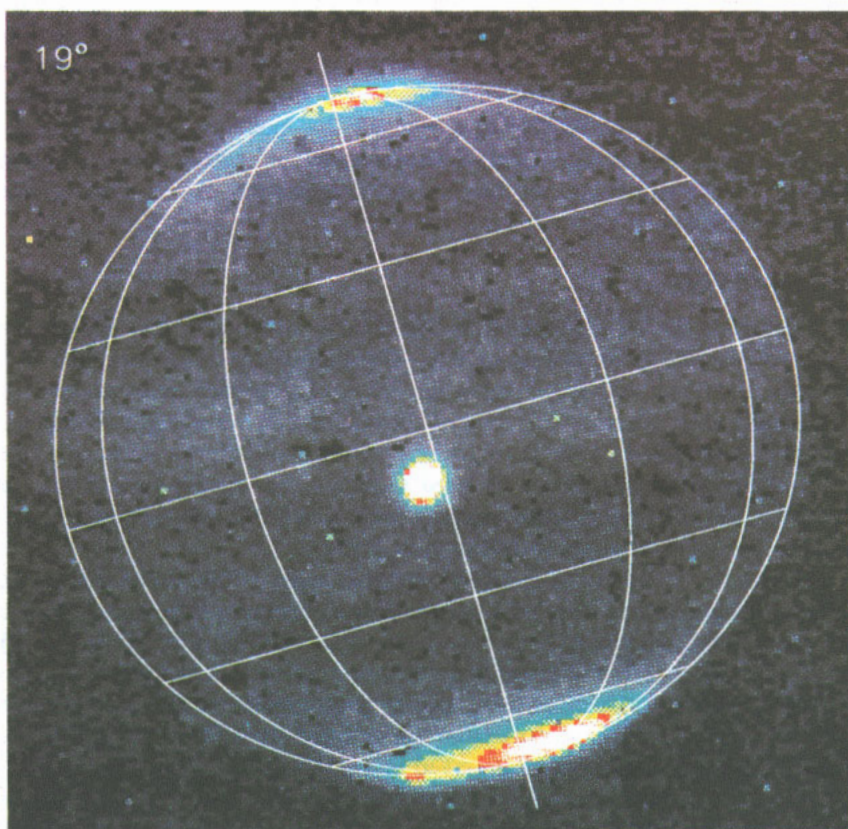


Figure 8. Infrared image of Jupiter with Ganymede passing at a wavelength sensitive to H_3^+ . The picture was recorded by Robert Joseph and Jonathan Tennyson in February 1991 using a 1% filter at $3.4 \mu\text{m}$ (2940 cm^{-1}) on the protoCAM imaging camera on NASA's Infra Red Telescope Facility (IRTF). The central white spots is one of Jupiter's moons, Ganymede, which is simply reflecting sunlight. On Jupiter this radiation is absorbed by gases, particularly methane, in the atmosphere. The colour scheme is used to denote the intensity of the emitted radiation. Lines of latitude and longitude have been superimposed on the raw image to show the position of the planet.

the H_3^+ emissions, hence Doppler widths and hence effective translational temperatures simultaneously with a rotational temperature. Both proved to be near 1200 K.

In fact detailed modelling by Kim *et al* (1992) showed that the impression that H_3^+ is in LTE must be treated with caution. In the low-density conditions of the Jovian ionosphere it is necessary to consider radiative cooling as well as collisions when considering the occupancy of the various states of H_3^+ . Kim *et al* found that the rates of radiative and collisional cooling of H_3^+ in its ν_2 and $2\nu_2$ vibrational states are approximately equal. They showed that, while the ratio of populations for these vibrationally excited states might give the appearance of LTE, radiative cooling leads to considerably more ground-state H_3^+ than might be expected from pure Boltzmann statistics.

It is not coincidence that a number of different H_3^+ effective temperatures have been mentioned in the above paragraphs. This is because observations taken at different times have recorded markedly different temperatures. Temperatures just above 1000 K would

appear to be most common, but values between about 670 K (Oka and Geballe 1990) and 1200 K (Drossart *et al* 1993) have been reported. Although some allowance must be made for systematic errors such as observing different regions or aspects of the planet, there is little doubt that these temperature fluctuations are real. Thus, for example, Oka and Geballe (1990) were completely unable to detect any $2\nu_2$ emission spectrum which, calculations suggest, should only be significant for temperatures above about 800 K. Furthermore, camera imaging of H_3^+ emissions, see below, also suggests that the strength of these emissions fluctuates (Kim *et al* 1991, Baron *et al* 1991).

7.3. Morphology

The detection of H_3^+ emissions in the Jovian ionosphere has provided an excellent spectroscopic handle on auroral activity. The ionospheric emissions of the H_3^+ fundamental have the additional advantage that in the $3.5 \mu\text{m}$ region they occur against the background of a totally dark planet. This occurs because at this wavelength all the incoming solar radiation is absorbed in the lower atmosphere, particularly by methane. This means that *infrared* imaging cameras can be used to picture the morphology of H_3^+ emissions, see figure 8. This itself has sparked much research which will only be summarized briefly here; a fuller discussion is given by Miller *et al* (1994).

Jupiter has a very large magnetic moment, some 10 000 times that of the earth. The resulting magnetic field thus has a very profound effect on a large region of space, stretching out some 100 Jovian radii from the planet. It is believed that H_3^+ is formed by charged particles spiralling into the planet at speed down magnetic field lines. These particles ionize molecular hydrogen which, in turn, leads to the formation of H_3^+ . It seems likely that these particles also provide the considerable energy input required ($\sim 10^{14}$ – 10^{15} W m^{-2}) to give the high effective temperatures observed in the H_3^+ spectra.

There are two possible sources of particles to travel down the magnetic field lines, the volcanos on Io and the steady stream of particles blown off the outer atmosphere of the sun. The Voyager mission confirmed the supposition that Io, the closest to Jupiter of its four large 'Galilean' moons, was volcanic (Morrison and Samz 1980). The gases emitted by these volcanos are spread out all round Io's orbit forming what is called the Io plasma torus.

Because the Io plasma torus is only about six Jovian radii away from the planet, particles spiralling along magnetic field lines enter the ionosphere at significantly lower latitudes than particles travelling on the open field lines which connect with the solar wind. Most of the indications (Baron *et al* 1991) are that the H_3^+ emissions are at too high latitude on the planet to be connected directly to the Io plasma torus. Detailed analysis by Connerney *et al* (1993) of a series of images similar to those in figure 8 showed most of the auroral emission was indeed confined to the high latitudes associated with open field lines and hence the solar winds. However in several images they were also able to detect a small emission region at lower latitudes. They were able to associate this feature directly with the position of Io which therefore leaves its footprint in the H_3^+ emissions seen on Jupiter.

Auroral activity on Jupiter has been observed in three different chemicals using three different wavelengths. Until recently the H_3^+ emissions in the near and mid *infrared*, the hydrocarbon emissions in the mid *infrared* and the *ultraviolet* emissions of molecular hydrogen all appeared to have markedly different morphologies. However, using the Hubble Space Telescope, Gerard *et al* (1993) have recently observed the H_2 auroral *ultraviolet* emissions with greatly improved spatial resolution. Their results show spectacularly good spatial correlation with the observed H_3^+ aurora which can now be assumed to be driven by the same mechanism.

Finally mention should be made of the H_3^+ airglow observed in the body of Jupiter. Weak emissions from the fundamental band of H_3^+ have been observed right the way across the planet by a number of groups (Oka and Jagod 1993, Ballester *et al* 1994, Marten *et al* 1994). These emissions are probably only about 10% of those observed in the polar regions. This has meant that spectral fitting to obtain reliable temperature estimates has proved more difficult, although temperatures are now generally believed to be somewhat lower than the polar region at about 800 K (Marten *et al* 1994).

It seems likely that this H_3^+ is either carried equatorwards from the poles by strong winds or arises as a result of photoionisation by solar *ultraviolet* radiation. The latter effect can be monitored because there is a measureable increase in the H_3^+ emissions on the setting side of the planet.

7.4. Impact of comet Shoemaker–Levy 9

During a week in July 1994 the 21 fragments of comet Shoemaker–Levy 9 plunged into Jupiter. This event was predicted more than a year in advance and was closely studied at all wavelengths. Observations performed on the United Kingdom Infrared Telescope (UKIRT) monitored impacts B and C (the second and third) at $3.5 \mu\text{m}$, a wavelength sensitive to H_3^+ . Impact B, which was a very minor one and largely unobserved by other telescopes, was clearly visible as an H_3^+ ‘flash’ as the cometary fragment passed through the Jovian ionosphere (Dinelli *et al* 1994b).

Impact C was altogether more spectacular with the H_3^+ emissions, usually the only species observable at $3.5 \mu\text{m}$, completely swamped by other features, in particular ones due to hot methane (Dinelli *et al* 1994b). Superficially the H_3^+ emissions were also greatly enhanced in the impact region but final conformation of this will have to await a more thorough analysis of the problem.

While UKIRT was looking at spectra, NASA’s Infra Red Telescope Facility (IRTF) was monitoring images (Orton *et al* 1995). Analysis of images in the $3.5 \mu\text{m}$ regions showed that several days after the impacts, which all occurred around 44° South, the southern aurora, as monitored by H_3^+ emissions, had dimmed while the northern aurora was significantly brightened (Miller *et al* 1995). This effect, which was also recorded in spectra taken with UKIRT, lasted for several days.

It is still early days in the analysis of collision data and the conclusions sketched above will possibly alter with further analysis. However, there is no doubt that H_3^+ spectra have again provided a valuable handle for monitoring activity in Jupiter’s ionosphere.

8. H_3^+ in the other giant planets

8.1. Detection in Uranus

The detection of H_3^+ on Jupiter naturally led astronomers to look for its characteristic spectrum in other giant planets. Saturn, the next largest and the next nearest of the giant planets after Jupiter, was the most obvious target. However, initial attempts to detect H_3^+ in Saturn by Geballe and co-workers in 1991 proved negative. It was therefore more in hope than expectation that Trafton *et al* (1993) used the stub end of a night devoted to observing Jupiter to take a look at Uranus.

What Trafton *et al* saw was perhaps one of the purest H_3^+ spectra ever recorded, see figure 9, with essentially no background and no emission from any other species. This spectrum was fitted using the parameters of Kao *et al* (1991) and gave a temperature of 740

± 25 K. Interestingly extrapolating this emission over the entire H_3^+ spectrum suggested that H_3^+ was emitting about 0.5×10^{12} W. This figure should be contrasted with the *total energy* required to power the aurora of 0.2×10^{12} W estimated by Broadfoot (1986) at the time of the Voyager 2 flyby. This seeming contradiction may actually be explained by the fact that the Voyager flyby took place during a period of relatively low solar activity, but during Trafton *et al*'s observations, the solar activity was close to its maximum.

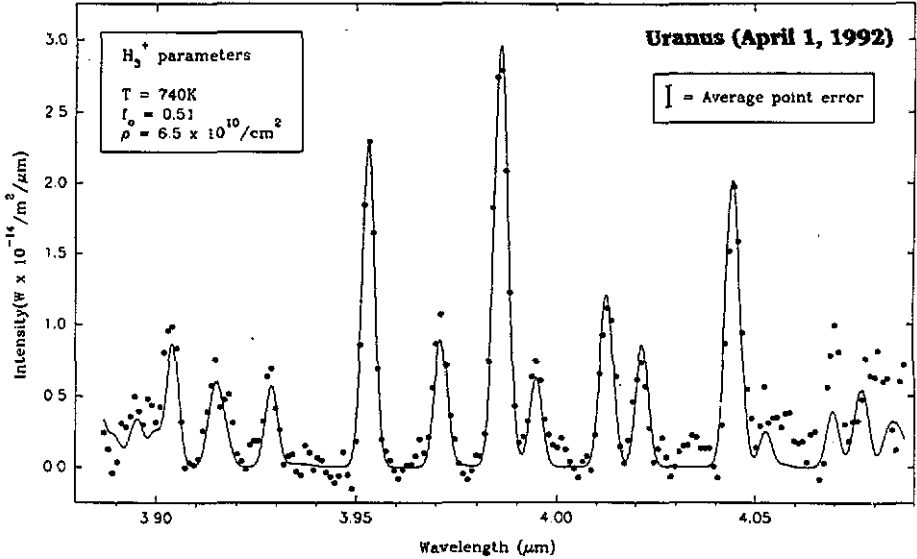


Figure 9. Emission spectrum of Uranus recorded by Trafton *et al* (1993) using the United Kingdom Infra Red Telescope (UKIRT). The dots represent the observed spectrum and the continuous curve is a theoretical H_3^+ spectrum with a (rotational) temperature of 740 K at the resolution of the telescope. In fact most of the peaks are blends of several H_3^+ lines. Note the absence of any other features and almost total absence of any background emission.

Using H_3^+ to probe the morphology of Uranus's ionosphere is much more difficult than for Jupiter as Uranus is both smaller and further away. Lam *et al* (1995) exploited exceptionally good 'seeing' to take a series of images in the 3–4 μm region. These images show H_3^+ emission all over the planet but also pronounced structure suggestive of enhanced auroral activity in a region about the magnetic pole. The current position of Uranus' magnetic pole is not known, so this analysis is, at the moment, conjecture. However, it is possible that H_3^+ could provide a unique observational handle on the position of Uranus' magnetic poles and hence also its period of rotation.

8.2. Saturn and Neptune

Three months after the detection of H_3^+ on Uranus it was eventually detected on Saturn by Geballe *et al* (1993). The lines detected were only 1% as bright as the corresponding Jovian emissions and were even weaker than those on Uranus. Analysis of Geballe *et al*'s spectrum suggested a temperature of about 800 K.

Comparisons of the flux of H_3^+ emission per unit area gives similar values for Jupiter and Uranus, but those from Saturn are some two orders of magnitude weaker. Why Saturn

has so much less H_3^+ activity is still not really understood. One suggestion is that its rings break up the flow of charge particles down the magnetic field lines and hence suppress auroral activity; another is that the hydrocarbons, particularly methane, in Saturn's upper atmosphere might act to rapidly destroy H_3^+ . Which, if either, of these suggestions is correct will have to await further work.

The night after their successful detection of H_3^+ on Uranus, Trafton *et al* (1993) attempted a similar observation for Neptune. Despite integrating for nearly an hour they were unable to obtain an identifiable H_3^+ spectrum, which places an upper limit on H_3^+ emissions considerably below that observed on Uranus. A subsequent, longer observation of Neptune by Geballe *et al* (1994) also failed to detect any H_3^+ emissions.

Given that Neptune is only a third the size of Uranus when viewed from Earth and that it receives a considerably reduced flux of particles from the solar wind, it is probably not surprising that any H_3^+ signature is weak. However, it is likely to be present and I would expect it to be detected in due course.

9. H_3^+ in emission outside the solar system

9.1. Background

As discussed in section 6, the attempts to observe H_3^+ absorption spectra in the ISM have thus far proved largely inconclusive. This difficult observation requires, amongst other things, a suitable star behind the object being observed to provide the continuum radiation for the molecules to absorb. With the observation of strong emission spectra in the giant planets, the idea grew that emission might be an easier and more fruitful way of detecting H_3^+ outside our solar system.

Emission spectra are strongly temperature dependent. For H_3^+ emissions it is necessary to have vibrationally excited states which require at least 2000 K of energy. These are likely to be undetectable in objects cooler than about 500 K. Experience with Jupiter shows that emissions from the overtone $2\nu_2$ band, which lie in the $2 \mu\text{m}$ region where detectors are generally more sensitive, cannot be observed from H_3^+ with an effective temperature lower than 700 K.

To observe H_3^+ emissions it is therefore necessary to have molecular gas at several hundred degrees. The emissions of molecular hydrogen, those originally sought by Drossart *et al* on Jupiter, have been recorded in many locations in the Universe (Genzel and Stutzki 1989). Observation of such emissions would appear to be a prerequisite for observing H_3^+ , but one further requirement would appear to be a source of ionizing radiation.

9.2. Supernova 1987a

In February 1987 a supernova, SN1987a, exploded in the nearby galaxy called the Large Magellanic Cloud. This event gave modern astronomers a so far unique opportunity to study the spectacular death of a massive star at close quarters. Observational programmes were rapidly constructed and, in particular, Meikle *et al* (1989) recorded *infrared* spectra of SN1987a at approximately fortnightly intervals. Meikle *et al* noted that this supernova was the first for which molecular emission features had been recorded and their spectra showed evidence for CO, CO^+ and CS, as well as a number of unassigned features.

The features that particularly caught the attention of Miller *et al* (1992) were those at 3.41 and $3.53 \mu\text{m}$ which were strongest about 200 days after the original explosion. These are exactly the wavelengths where H_3^+ emissions are so prominent in Jupiter. Furthermore

these features were too broad to be due to single lines, and blends which might be expected for hot, Doppler broadened H_3^+ , seemed to be likely. Detailed fits to these features, see figure 10, gave temperatures around 2000 K but a rather large uncertainty as, amongst other things, it is necessary to make rather crude assumptions about the level of background radiation before fitting can be attempted. The situation is further complicated by the possibility that the central structure in the $3.41 \mu\text{m}$ feature may be due to atomic sodium (Lucy *et al* 1991).

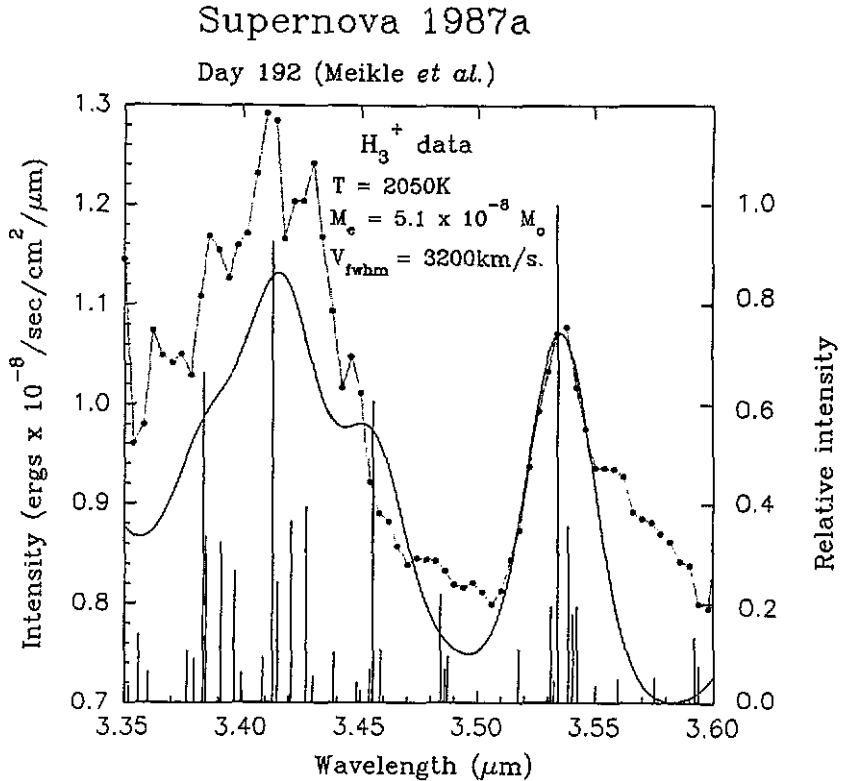


Figure 10. Fit of the computed $\text{H}_3^+ \nu_2 \rightarrow 0$ spectrum (full curve) to the Day 192 L window spectrum of Supernova 1987a (filled circles) from 3.35 to $3.60 \mu\text{m}$ by Miller *et al* (1992). The vertical lines represent the individual transitions used in the fit.

Chemical modelling performed in parallel with the spectral analysis suggested that significant quantities of H_3^+ could be produced provided that microscopic mixing did not occur in the supernova ejecta. Interestingly, calculations using the now discredited slow dissociation recombination rate for H_3^+ (see section 3.2) suggested that so much H_3^+ would be produced that the entire spectrum in the $3\text{--}4 \mu\text{m}$ range would be dominated by it.

The assignment of H_3^+ in SN1987a made by Miller *et al* (1992) is not universally accepted (e.g. Watson 1993), but no other plausible candidate(s) have been suggested for the emission features at 3.53 , 3.36 and $3.41 \mu\text{m}$. As day 200 hundred of SN1987a has long gone, astronomers may have no alternative but to wait a few centuries for another supernova as bright as SN1987a to provided the necessary confirmation. However, there is hope that technological advances may mean that equivalent spectra will be recorded for more distant supernovae in the near future (Oka 1993, Black 1993), thus sparing us the wait.

9.3. Emissions from other sources

Observations from other possible sources of H_3^+ emission both in our galaxy and outside have proved somewhat inclusive (Tennyson *et al* 1993, Schild *et al* 1994). However, recently Hibbins *et al* (1994) have made a very interesting suggestion that the H_3^+ feature at $3.53 \mu\text{m}$ might be differentially pumped by hydrogen atom Brackett- α emission at $4.05 \mu\text{m}$. Using this idea they are able to produce model spectra for H_3^+ with a rotational temperature of about 300 K which are, in the $3\text{--}4 \mu\text{m}$ region, completely dominated by a doublet centred on $3.53 \mu\text{m}$. Furthermore they demonstrate that this feature is plausibly like ones observed previously in the star forming regions Elias 1 (Tokunaga *et al* 1991) and DH97048 (Schutte *et al* 1990).

This proposal needs testing further and would be considerably strengthened by an observation which could resolve the doublet at $3.53 \mu\text{m}$. However, Hibbins *et al* note that there are a number of other objects which display the $3.53 \mu\text{m}$ feature. They also note that the effects of pumping were not included in the model of the spectrum SN1987a discussed above, and that including pumping should remove some of the discrepancies with this assignment too.

10. H_3^+ at its dissociation limit: laboratory spectra

10.1. The original observation

In 1982 Carrington, Buttenshaw and Kennedy published a brief research note in *Molecular Physics* announcing the observation of a very unusual photodissociation spectrum for the H_3^+ molecular ion. These workers made H_3^+ using electron impact ionization of H_2 , selected these ions with a mass spectrometer and photodissociated them using a CO_2 laser:



Photodissociation was monitored using an electrostatic analyser (ESA) which was set to monitor the proton current. The ESA is also sensitive to the kinetic energy of the ions monitored and the original spectra were obtained by observing those ions with approximately zero kinetic energy in the framework of the molecule.

Simplistically, the kinetic energy released in the molecular frame corresponds to the amount of energy above dissociation contained by the fragmenting ion. However, the situation is complicated by the fact some of the excess energy can be carried away by the molecular hydrogen fragment as vibrational or rotational excitation. Furthermore, the ESA only gives approximate kinetic energy resolution and protons with a range of kinetic energies are in practice expected to contribute to the spectrum.

The experimental set up of Carrington and co-workers is very sensitive; their spectrum results from between 0.1 and 1% of the ions in their system (Carrington and Kennedy 1984). However, Carrington *et al* observed a very large number of well defined transitions in the limited range of their laser, $872\text{--}1094 \text{ cm}^{-1}$. As the dissociation energy of H_3^+ is about $35\,000 \text{ cm}^{-1}$ (Cosby and Helm 1988, Lie and Frye 1992), this experiment monitored only those levels of the ion which lay very close to the dissociation limit. Prior to this experiment the structure of the rotation-vibration energy levels at dissociation for chemically bound molecules larger than diatomic was completely unknown. Indeed H_3^+ and its isotopomers remains the only strongly bound polyatomic which has been studied in this fashion.

Carrington *et al*'s spectrum was unexpected and truly remarkable. It stimulated my interest in the H_3^+ molecular ion and has also spawned a whole host of other theoretical work on the near-dissociation problem which will be discussed in the following sections.

10.2. Detailed spectrum and its coarse-grained structure

Carrington and Kennedy (1984) gave a detailed account of the photodissociation spectrum; this included reporting nearly 27 000 transitions in the 222 cm^{-1} spanned by their laser. These discrete lines had widths which varied between 3 MHz (0.0001 cm^{-1}), the Doppler width in their experiment, to several hundred MHz. This and other tests (see McNab 1995) showed that this spectrum was indeed due to photodissociation.

Carrington and Kennedy's and the earlier spectra were obtained at very high resolution. Indeed with their set up it was not possible to obtain low-resolution spectra. However, Carrington and Kennedy performed computational experiments which synthesized low-resolution spectra. They took their observed line list and artificially broadened it. The most interesting spectrum they obtained was generated by convoluting the 1934 most intense transitions with a Gaussian linewidth of 4 cm^{-1} . This pseudospectrum gave four 'peaks', I prefer the description 'clumps', at 876, 928, 978 and 1034 cm^{-1} . Other convolutions also showed the same four features. This coarse-grained regularity with a period of about 50 cm^{-1} is an important feature and the one upon which most theoretical effort has concentrated.

Carrington *et al* (1993) repeated Carrington and Kennedy's coarse-graining procedure using their new, improved dataset of lines. Using a Gaussian linewidth of only 2 cm^{-1} , they found that the clump at 978 cm^{-1} could be clearly resolved into a quartet with intensities in the ratio 1:3:3:1. At this resolution the other clumps appeared as poorly resolved doublets. As yet there are no theoretical explanations for this further observed structure.

10.3. Lifetimes of the states involved

Carrington and Kennedy (1984) performed a number of other experiments. For example, tuning their ESA to monitor kinetic energy releases in excess of 3000 cm^{-1} , significantly more than the energy on their incoming photons, they were still able to observe a clear spectrum. This demonstrated that, for at least some of the ions involved, both the upper and lower states involved in transitions lay above the H_3^+ dissociation limits and were thus only quasibound.

Chemists usually refer to quasibound levels found in spectra as predissociating. Predissociation spectra have characteristic linewidths due to the uncertainty principle as their finite lifetime ($\Delta\tau$) is linked to the energy resolution with which they can be observed (ΔE) by $\Delta E\Delta\tau \geq \hbar/2$.

Rotating molecules display a barrier to dissociation which increases with rotational angular momentum. Predissociation by tunnelling through such a barrier is well known and it is this that Carrington and Kennedy concluded that they were observing. Physicists commonly refer to quasibound states trapped behind angular momentum barriers as shape resonances. Because of the density of transitions observed it seemed likely that the H_3^+ states involved would be highly rotationally excited.

Any theory which attempts to explain the Carrington-Kennedy experiment must allow for the lifetime considerations introduced by the experimental set up itself. For ions to reach the drift tube irradiated by the CO_2 laser it is necessary for them to live at least a microsecond. Conversely, if the excited ions are to fragment quickly enough to be detected by the ESA it must have a lifetime of less than about $0.7\text{ }\mu\text{s}$. However, ions which fragment very quickly, with lifetimes less than about 7 ns, give lines which are too broad to be detected against the background noise.

Carrington *et al* (1993) analysed further the lifetime constraints in their experiment. Lifetimes were measured directly for a few initial states and results in the 1-2 μs

region found. Detailed analysis of their line profiles suggested that the excited states all had lifetimes in the range 0.5–20 ns, slightly shorter than those predicted previously. Interestingly, they also found that the more intense transitions they measured correlated with longer living upper states. This observation is consistent with theoretical models of the spectrum arising from transitions to a bright gateway state which is coupled to a bath of other nearby states (see Le Sueur *et al* 1993).

Further discussion of the experimental procedures used can be found not only in the original articles (Carrington *et al* 1982, 1993; Carrington and Kennedy 1984) but also in the reviews of Carrington and McNab (1989) and McNab (1995).

10.4. Isotopic substitution

Besides H_3^+ , Carrington and Kennedy (1984) also recorded the near-dissociation spectra of H_2D^+ , D_2H^+ and D_3^+ . For D_3^+ , they found a spectrum which was both weaker and denser than that of H_3^+ .

The most interesting spectra were those of the mixed isotopomers as for these it was possible to use either protons or deuterons as the means of detection. As it is difficult to discriminate between H_2D^+ and D_2H^+ using a mass spectrometer, Carrington and Kennedy performed their most detailed work on D_2H^+ .

For D_2H^+ , Carrington and Kennedy found that monitoring D^+ gave a significantly weaker spectrum than that obtained by monitoring H^+ . Furthermore the spectra, which were recorded at zero kinetic energy release, were completely different. It should be noted that the H^+ dissociation channel lies below the D^+ channel by 371 cm^{-1} because the zero-point energy of D_2 is lower than that of HD .

To my knowledge no-one has ever constructed coarse-grained spectra of the mixed isotopomers. Given the heavy reliance placed on reproducing the coarse-grained spectrum of H_3^+ in nearly all theoretical studies, these spectra could provide valuable constraints on any theoretical model. However, it would take several years of work to accumulate the necessary data using the experimental set up employed by Carrington and co-workers.

Theoretical analysis of the mixed isotopomers (Berblinger *et al* 1988a, 1989, Chambers and Child 1988) showed that there should be a strong correlation between kinetic energy release and dissociation. In particular, for D_2H^+ , it was suggested that protons should only be produced with kinetic energies below 680 cm^{-1} and deuterons should only occur above 286 cm^{-1} . Carrington *et al* (1993) test these predictions and found that their observations were completely compatible with them.

Carrington *et al* (1993) also analysed the 'noise' in their experiment, i.e. the background current of protons (deuterons) obtained either with no laser or the laser tuned to a non-resonant frequency. This observation is sensitive to ions which spontaneously fragment (predissociate) in their drift tube. Tests on the kinetic energy release of protons and deuterons from D_2H^+ again produced results consistent with the theoretical predictions.

10.5. Spectra at high kinetic energy release

Carrington *et al* (1993) published the results of further major studies on the H_3^+ near-dissociation spectrum. They demonstrated the reproducibility of their results, which had been questioned, and considered other possible defects of their earlier experiments. They also obtained spectra using considerably lower laser power which meant that they did not have problems with saturation effects.

Most of the previous spectra obtained by Carrington and co-workers had been obtained at zero kinetic energy release although for all isotopomers it was possible to obtain spectra

for kinetic energy releases significantly greater than the incoming photon. Carrington *et al* (1993) presented the results of spectra obtained as a function of kinetic energy release.

Given the time consuming nature of their experiments, Carrington *et al* chose to only study in detail the frequency region (964.0–991.6 cm^{-1}) which contributed to the coarse-grained peak at 978 cm^{-1} . They found that initial increases in the kinetic energy release monitored gave an even denser spectrum. Indeed their spectra for a release of 500 cm^{-1} could superficially be mistaken for noise except that the results are highly reproducible.

At high kinetic energy release (3000 cm^{-1}) Carrington *et al* observed spectra with a few, strong transitions. As the high kinetic energy release spectra can only arise from initial states which lie well above the dissociation limit, this observation suggests that these states are somehow more regular (see below) than the lower energy states which dominate the zero kinetic energy release spectra.

Carrington *et al* (1993) made an attempt to make a partial assignment to some transitions by seeing whether the same H_3^+ transition could be observed at significantly different kinetic energy releases. Such an observation would imply that different vibration–rotation levels of H_2 were being produced by fragmentation of the same excited state. Assignment of the H_2 states by their energy difference could also lead to partial assignment of the excited state in question. Several states undergoing multichannel dissociation were identified, but unfortunately the measurement of the kinetic energy released was too crude to allow for assignment of the associated states of H_2 .

With publication of their final comprehensive analysis of the H_3^+ near-dissociation spectrum, Carrington *et al* (1993) concluded their experimental exploration of this highly unusual spectrum. Instead they appealed for theoretical assistance in interpreting their results. The last decade has indeed seen considerable theoretical activity in this area. However, in the terms that spectroscopists usually understand high resolution spectra the spectrum remains a complete mystery: not a single transition has had any quantum numbers assigned to it.

11. H_3^+ at its dissociation limit: (semi)classical studies

11.1. General considerations

The spectra reported by Carrington *et al* (1982) and Carrington and Kennedy (1984) were completely unexpected; no theoretical models existed to explain the observations. In particular answers to the following questions were urgently required:

- (i) Why were the states so long lived?
- (ii) Why were there so many transitions in such a small spectral region?
- (iii) What was the cause of the coarse-grained structure?
- (iv) How could the H^+ and D^+ spectra for the mixed isotopomer be explained?

H_3^+ is a quantal system in which coupling between the modes was known to be strong. However, initially most work used classical or semiclassical analysis. This situation arose partly because it was simply not possible to perform accurate quantal calculations at the dissociation limit of a strongly bound triatomic such as H_3^+ and partly because the initial studies focused on gaining insight into the nature of the spectrum rather than a full numerical treatment of the problem. Indeed there is a large body of work on the (semi)classical treatment of the dynamics of small molecules (Child 1991). Although the Carrington–Kennedy spectrum has acted as a tremendous stimulus to theory, a full quantitative treatment of the problem remains some way off.

11.2. Lifetimes

On molecular time scales the lifetimes involved in the fragmentation of the H_3^+ ion are lengthy. For example simple application of the standard theory used to explain unimolecular break-up, the so called RRKM theory (Murrell and Bosanac 1989), would predict that the excited fragment with excess energy in the 2000–3000 cm^{-1} range would dissociate inside 3 ps (Schlier and Vix 1985, Pollak and Schlier 1989). Similarly the strong vibrational coupling found in the system means that states with excess vibrational energy, which can be regarded as Feshbach resonances, decay much too quickly to be significant (Pollak and Schlier 1989, Drolshagen *et al* 1989). Attention therefore immediately focused on quasibound states trapped behind a rotational barrier or shape resonances.

For a non-linear polyatomic molecule even quantifying the rotational barrier is not straightforward. This is because Coriolis effects give rise to different effective barriers for different arrangements of the atoms in the molecule. In H_3^+ the extreme and critical cases are when one atom is perpendicular to the mid-point of the other two in an isosceles triangle and when the molecule is linear. Pollak (1987) treated the triatomic rotational barrier problem by defining an effective potential which followed an effective reaction coordinate along the minimum energy pathway for fragmentation. His classical procedure made predictions for the highest values of the rotational angular momentum of the system which were later confirmed by quantal calculations (Miller and Tennyson 1988a).

In classical mechanics, of course, a state trapped behind a potential barrier will never decay. In order to estimate decay lifetimes it was therefore necessary at least to obtain quantal estimates of the probability of tunnelling through the barrier. Gomez Llorente and Pollak (1988) obtained estimates of the decay time for H_3^+ using the classical tunnelling trajectory (CTT) method. Their rates for unimolecular decomposition were deemed consistent with the lifetimes observed in the Carrington–Kennedy experiment but were actually at the short end of the range and obtained for high angular momentum ($J \sim 40$). Gomez Llorente and Pollak (1989) considered lower angular momenta and obtained somewhat longer lifetimes.

The CTT method estimates the frequency of collisions with the barrier using classical trajectory calculations and allots each trajectory a tunnelling probability by solving a one-dimensional (1D) tunnelling problem for each collision. The main drawback of this procedure is that it is possible to obtain products with energy less than their zero-point energy. This is a significant problem in the dissociation of H_3^+ as the zero-point energy of H_2 is considerable ($> 2000 \text{ cm}^{-1}$).

Berblinger *et al* (1988b, 1989) estimated decay times using a sudden transition state theory (TST). This method is computationally quicker but inherently less accurate than the CTT method. However, it can be regarded as complementary as sudden TST can be formulated to remove zero-point effects. As CTT lifetimes, with zero-point corrections, and sudden TST results were found to be in good agreement, this gave some confidence in the results.

Recently Berblinger and Schlier (1994) tested classical RRKM theory for D_2H^+ unimolecular dissociation as a function of total angular momentum and energy above dissociation. They found that non-ergodic (i.e. non-chaotic) directly dissociating trajectories led to a 40% increase in the rate over RRKM theory but that without these trajectories the RRKM predictions were reproduced within the accuracy of their calculations.

An alternative explanation for the observed long H_3^+ lifetimes has been given by Quack (1990) who focused on the unimolecular decay of H_3^+ vibrational levels with A_2 symmetry. These states have nuclear spin $I = \frac{3}{2}$ and thus have no direct channel into $H_2(v, j = 0) + H^+$ without flipping one nuclear spin. This process could therefore take microseconds. This

explanation would appear to ignore the observation that lifetimes of similar lengths were recorded for all the isotopomers studied by Carrington and co-workers. Quack's explanation has not been pursued and the model of tunnelling through a rotational barrier is now generally accepted.

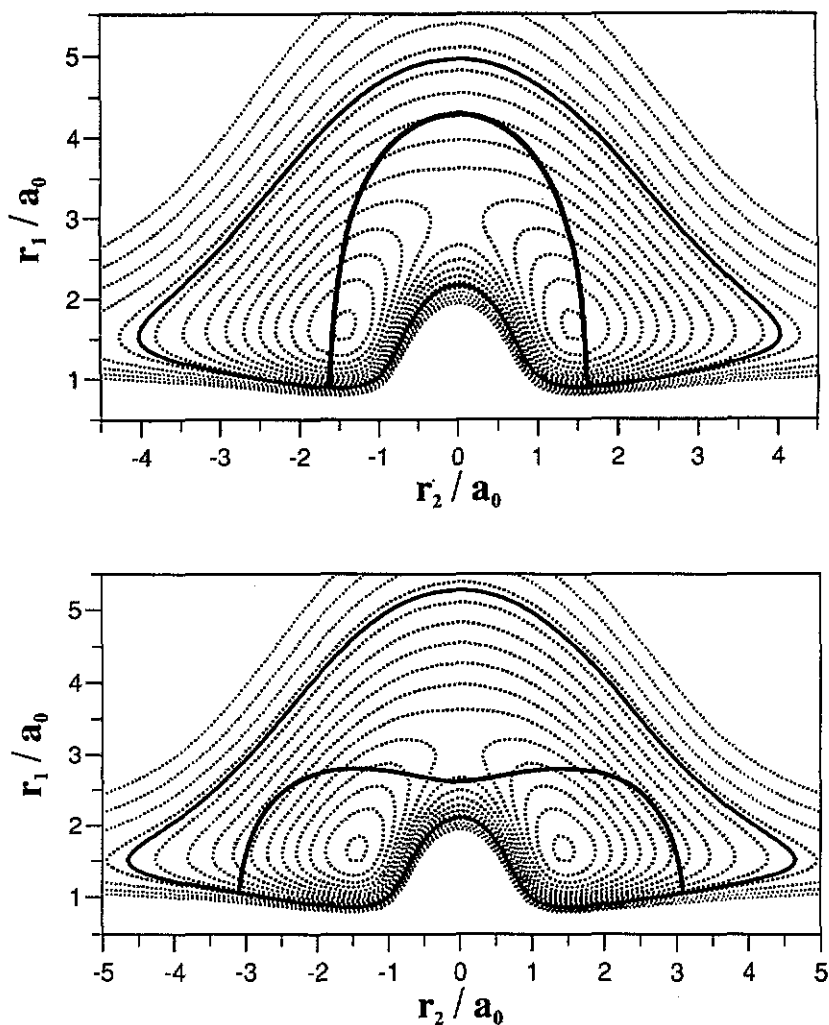


Figure 11. Classical periodic orbits: upper one the 'horseshoe'; the lower one the 'elephant's foot'. The contours are the H_3^+ potential with the bold one corresponding to the classical turning point of the periodic trajectory shown. The plots are all in scattering coordinates with θ fixed at 90° and are from Fulton (1994).

11.3. Density of states

Perhaps one of the most surprising things about the Carrington–Kennedy spectrum was the sheer density of transitions observed. The density of states in the dissociation region has been estimated semiclassically by computing the volume of the available phase space (the space spanned by both the position and momentum coordinates of the system) using

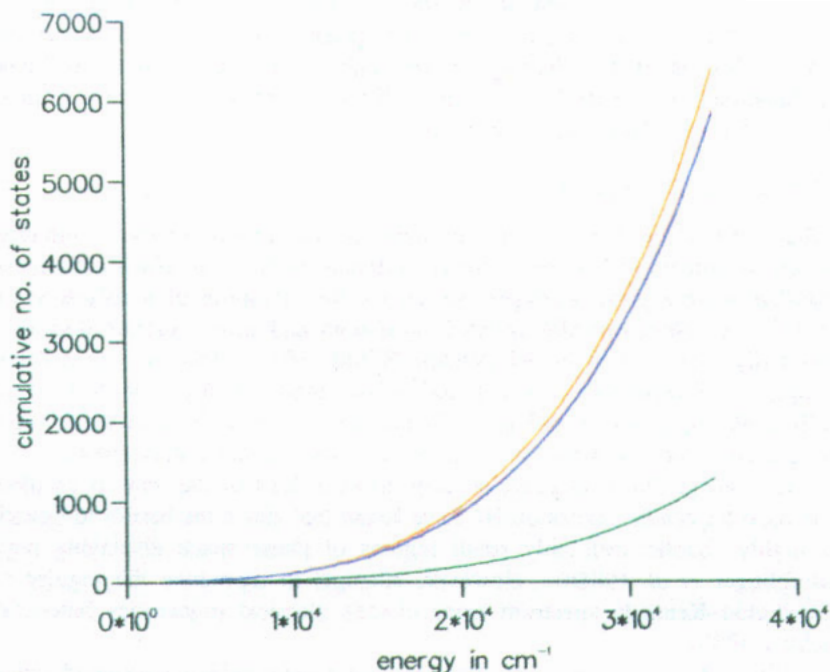


Figure 12. Density-of-states plot for H_3^+ for $J = 2$ and $J = 0$. The total number of states below a certain energy are plotted. Green curve, quantum calculation of Henderson *et al* (1993) for $J = 0$; blue curve, quantum calculation of Henderson and Tennyson (1995) for $J = 2$; orange curve, $2J + 1 = 5$ multiplied by the $J = 0$ curve; red curve, $(2J + 1)\sigma = 5\sigma$ multiplied by the $J = 0$ curve where $\sigma = 0.91$ is the semiclassical ratio between $J = 2$ and $J = 0$ density of states obtained by Berblinger and Schlier (1993). The excellent agreement between quantal and semiclassical estimates means that the red and blue curves lie on top of each other.

numerical integration. For a rotating triatomic molecule this requires evaluating an eight-dimensional integral numerically. This was done by Berblinger *et al* (1988b) for H_3^+ for values of J which had quasibound states ($J \leq 74$) using Monte Carlo integration at the rate of one J level per day on their computer to give an accuracy of $\sim 2\%$.

Subsequently Berblinger and Schlier (1992) were able to reduce the dimensionality of the integral that needed to be evaluated numerically leading to greatly enhanced computational efficiency. Comparison of their results with full quantum mechanical calculations for rotationless H_3^+ showed excellent agreement up to $35\,000\text{ cm}^{-1}$, the range of validity for the quantal calculations (Berblinger *et al* 1992). Unpublished calculations for rotationally excited H_3^+ show similarly good agreement between the semiclassical predictions of Berblinger and Schlier, and the quantal calculations of Henderson and Tennyson, see figure 12. As H_3^+ is probably the least classical molecule for which such densities of states are of interest, these comparisons suggest that using phase space integration to generate densities of states near dissociation is a much more reliable procedure than other methods, for example based on sums of harmonic states, presently being used.

The calculations of Berblinger *et al* (1988b) suggested that, summed over all J , H_3^+ has some 80 000 bound or quasibound states. This is clearly more than enough to give 27 000 transitions. Indeed only $\sim 2\sqrt{27\,000} \approx 330$ states are actually required to give the Carrington–Kennedy spectrum. However, besides obvious selection rules and energy

restrictions on the location of the states involved in this spectrum, detailed analysis of the experiments has pointed towards a number of severe constraints on the participating states. This means that, despite the seemingly large excess of states available, some of the explanations offered for the Carrington–Kennedy spectrum still have difficulty accounting for the density of observed transitions.

11.4. Structure of phase space

‘Chaos theory’ has been a recent hot topic in mathematical physics. One particular class of problems studied are conservative Hamiltonian systems of which anharmonically coupled oscillators are a prime example. Of course the vibrations of a polyatomic molecule such as H_3^+ are anharmonically coupled oscillators and these systems display many features originally identified in model systems (Child 1991). However, most detailed studies of coupled oscillators have concentrated on two-mode problems because of the difficulty of fully exploring problems of higher dimensionality. Similarly many studies on the H_3^+ system have used reduced dimensions (e.g. Gomez Llorente and Pollak 1989).

H_3^+ can go linear at energies only about a third of the way to its dissociation limit. Classical trajectory studies on H_3^+ have found that above the barrier to linearity, the system is highly chaotic with only small regions of phase space displaying regular structures (Berblinger *et al* 1988b). However, attempts to reproduce the regular features of the Carrington–Kennedy spectrum using chaotic classical trajectories failed (Berblinger and Schlier 1988).

Given the high degree of chaos and new ideas which associated regular features in disordered spectra with quasiperiodic classical motions (see for example Gomez Llorente *et al* 1989), the search was on for regular features in the H_3^+ phase space. Because there is no general algorithm for finding regions of quasiperiodic motion in phase space, most searches have concentrated on analysing phase space in reduced dimension. In particular the problem with no rotational motion and one H atom constrained to move along a line cutting the mid-point of the other two H's (θ fixed at 90° in the coordinates of figure 4) has received particular attention. It should be noted that in this T-shaped geometry H_3^+ always has at least C_{2v} symmetry. One effect of this is that a classical trajectory started in such a geometry and moving only in r_1 and r_2 (see figure 4) will remain trapped in the T-shaped geometry even for a full (3D) calculation.

Berblinger *et al* (1988b) conducted an exhaustive study of T-shaped H_3^+ . They discovered a stable periodic orbit, which they called a ‘horseshoe’, which involved the unique H atom passing between the other two atoms, see figure 11. The horseshoe periodic orbit was the only significant periodic motion they discovered which remained stable in 3D. They thus dismissed the possibility of other periodic motions existing either in the T-shaped geometry or the full 3D coordinate space of H_3^+ . Berblinger *et al* found that the volume of phase space occupied by the horseshoe orbit was very small; indeed too small to quantize using standard semiclassical quantization procedures (Gomez Llorente and Pollak 1989).

Figure 15, which will be discussed further below, shows a cut through phase space, known as a Poincaré surface of section, for T-shaped H_3^+ in a near linear configuration. The regular structures in the centre of the figure are due to the horseshoe periodic orbit. The dots, which appear to fill the rest of the surface of section, are the hallmark of chaotic trajectories.

Gomez Llorente and Pollak (1989) further investigated the horseshoe and found that it was stable to rotational excitation. They found that the rotating horseshoes displayed effective rotational constants in the plane of the molecule with $2B \approx 60 \text{ cm}^{-1}$, which they likened to the 50 cm^{-1} spacing between the clumps in the Carrington–Kennedy spectrum.

Furthermore Gomez Llorente and Pollak identified another ('antisymmetric stretch' or ν_3) mode in their 3D classical spectra with a frequency of 643 cm^{-1} . This antisymmetric stretch formed the basis of a tentative assignment of the coarse-grained structure in the Carrington-Kennedy spectrum to R(3)-R(6) transitions of this mode.

Gomez Llorente and Pollak's (1989) assignment is by the far the most specific one made to the Carrington-Kennedy spectrum, but cannot yet be regarded as proven. There has been considerable further work on this problem, using both quantum and classical mechanics, see next section. The existence and strength of the horseshoe motion is beyond doubt. However, no other work has identified the antisymmetric stretching mode which is crucial to Gomez Llorente and Pollak's interpretation of the spectrum. Furthermore, the description of this mode as ν_3 and other aspects of their assignment would appear to ignore the rather high symmetry of H_3^+ which can cause quantum horseshoes to display somewhat different characteristics to the simple picture of figure 11 (Polavieja *et al* 1994b).

As discussed in section 12, quantal calculations (Tennyson *et al* 1990a, Polavieja *et al* 1994b) have revealed a number of other regular features which were found to have quasiperiodic classical analogues at T-shaped geometries. Furthermore, unpublished classical calculations by Child and co-workers have found interesting 'spiral' orbits in rotating 3D H_3^+ . The true significance of these and other orbits for the near dissociation spectrum of H_3^+ remains to be fully tested.

11.5. Angular momentum barriers

One aspect of the near-dissociation spectrum that theory has successfully explained is the behaviour with respect to isotopic substitution. Using Pollak's (1987) definition of an effective centrifugal barrier for a rotating triatomic, Berblinger *et al* (1988a, 1989) studied the minimum effective potential energy surfaces as a function of rotational excitation for H_3^+ and, more particularly, for the mixed isotopomers H_2D^+ and D_2H^+ .

Berblinger *et al* (1988a, 1989) found that what they described as J -dependent geometric isomers: for low J H_3^+ and its isotopomers favour a T-shaped geometry, but for some value of J the lowest-energy form becomes linear. Furthermore for the mixed isotopomers they found that the height of the centrifugal barrier depended on the dissociation channel. At low J , zero-point energy effects favour proton emission for both H_2D^+ and D_2H^+ . However, at high J , $J > 30$ in the case of D_2H^+ , emission of deuterons is preferred as this leads to significantly smaller barriers. These observations provide strong evidence that the experiments of Carrington and co-workers largely sampled molecules which had rotational angular momenta of $J = 25$ or less.

Chambers and Child (1988) reached similar conclusions about the effects of rotational excitation on the dissociation routes of the mixed isotopomers. Chambers and Child (1988) and Gomez Llorente and Pollak (1988) suggested a correlation between kinetic energy release and total angular momentum. This arises because most tunnelling occurs fairly near the top of any centrifugal barrier, the J dependence of the centrifugal barrier can also be used to estimate the kinetic energy release associated with a particular J level. In other words high kinetic energy release should correspond to states with high rotational angular momentum.

The proposed correlation of high kinetic energy release with high J gives an interpretation of the high kinetic energy release spectra. These spectra show many fewer lines which are significantly stronger than those observed at low kinetic energy release. Carrington *et al* (1993) rationalized this by arguing that the low kinetic energy release (low J) spectra arose from chaotic states and hence were dense with few dominant features, while the high kinetic energy release (high J) spectrum arises from states which are more

regular giving rise to a sparser, sharper spectrum. The idea that high J levels behave more regularly than those at low J is based on the fact that rotational excitation increases the saddle point at linear geometries. This saddle point is the anharmonic feature driving the onset of chaos and is increasingly blocked off as J increases (Brass *et al* 1990).

12. H_3^+ at its dissociation limit: quantal studies

12.1. The challenge and early attempts to meet it

H_3^+ is a deceptive system: because it only has two electrons and one bound electronic state it is easy to assume that calculations should be facile. However, as should be apparent from the classical calculations discussed in the previous section, the relatively low barrier to linearity leads to an irregularity in the vibration-rotation states of the system which it is very difficult to model theoretically. The density of these states also rises rapidly above this barrier.

At low energies, where conventional vibration-rotation spectra are recorded, basis set methods have been outstandingly successful for H_3^+ , see sections 4 and 5. However, early attempts to extend these methods blindly to the intermediate or high-energy regions were shown by Tennyson and Sutcliffe (1984) to be futile. New techniques were clearly required.

Carrington and Kennedy (1984) originally explained their spectrum in terms of the relatively simple H^+-H_2 Van der Waals complex. This explanation was based on a simple view of how molecules behave as they dissociate and the coincidence of the four coarse-grained features observed in their spectrum and corresponding transitions in H_2 .

Quantal (Pfeiffer and Child 1987, Drolshagen *et al* 1989) and classical (Gomez Llorente and Pollak 1987) calculations were performed within this model. These calculations, however, failed to explain a number of features of the observed spectrum, in particular the coarse-grained structure and the higher frequency transitions (Pfeiffer and Child 1987). They were abandoned with the growing realization that the strong mode coupling in H_3^+ meant the separation of vibrational motions implied in the Van der Waals complex model was unrealistic.

Given the difficulty of performing full calculations in the region of dissociation, attempts were made to solve relevant problems of lower dimension. Gomez Llorente *et al* (1988, 1989) used directly the insights given by classical calculations by placing Gaussian functions along trajectory of the horseshoe periodic orbit. Their calculations showed that wavefunctions did indeed localize about the horseshoe orbit; however it is hard to see, given the way the calculation was constructed, that any other results could be obtained.

Tennyson *et al* (1990a) performed quantal calculations on the 2D T-shaped structure studied classically by Berblinger *et al* (1988b) and others. These calculations showed clear evidence for the horseshoe states and also a new 'inverse hyperspherical mode'. This latter mode was duly identified in parallel classical calculations but was found, classically, not to be stable in 3D. Interestingly Tennyson *et al* estimated 'the' rotational constant of all the states in their calculation and found $2B \approx 60 \text{ cm}^{-1}$ for all states, not just the horseshoes as assumed by Gomez Llorente and Pollak (1989).

Brass *et al* (1990) extended Tennyson *et al*'s quantum-classical comparison to full 3D calculations. Although the quantum mechanical calculations were not converged, they still showed horseshoe structures in strikingly good agreement with the parallel classical calculations.

12.2. Vibrational states at dissociation

The Carrington–Kennedy spectrum has provided a tremendous stimulus for developing methods for performing calculations on high-lying vibrational levels. H_3^+ has become the benchmark molecule for which new methods can be assessed (see Wei and Carrington 1994 for example). Although very accurate energy levels for the vibrational states of H_3^+ are now available all the way to dissociation (Bramley *et al* 1994), this situation has been hard won with a number of disputed results along the way.

As implied above, it required a major change in the theoretical approach before serious calculations on the high-lying states of H_3^+ could be attempted. This was provided by the DVR originally proposed by Harris *et al* (1965) and rediscovered by Light and co-workers (see Bačić and Light 1989). Symmetry considerations make H_3^+ more difficult to treat in a DVR than some other systems; Light's group obtained excellent results for several other triatomics (Bačić and Light 1989) before turning their attention to H_3^+ .

Initially Whitnell and Light (1988) developed a method of symmetrizing a DVR calculation by developing DVR grids in symmetrized coordinates which they then applied to H_3^+ . Whitnell and Light (1989) obtained the lowest 60 energy levels of H_3^+ using the MBB (Meyer *et al* 1986) potential energy surface. The majority of these states lie above the barrier to linearity; the first time this region had been successfully treated in a full 3D quantal calculation. Whitnell and Light's method was considerably more reliable for non-degenerate (A_1 and A_2) vibrational states for which they obtained a further 20 levels.

Tennyson and Henderson (1989) adopted the DVR for treating the θ coordinate in the scattering coordinates, see figure 4, used for earlier calculations (Tennyson 1986). These coordinates cannot represent the full H_3^+ symmetry and C_{2v} symmetry was included by symmetrizing the DVR grid points. Tennyson and Henderson obtained energies and wavefunctions for the 180 lowest vibrational states on the MBB potential. They analysed their wavefunctions graphically and found evidence not only for states which were strongly localized about the horseshoe periodic orbit, but also for states showing vibrational excitation in a mode perpendicular to the horseshoe orbit. However, this excitation was in the r_1 – r_2 plane, unlike the antisymmetric stretch of Gomez Llorente and Pollak (1989), discussed above, which involves excitation in the θ coordinate. Tennyson and Henderson also found evidence for the inverse hyperbolic mode identified originally in 2D calculations by Tennyson *et al* (1989) but dismissed because of its lack of stability in 3D classical calculations.

Carter and Meyer (1990) used the MBB potential, hyperspherical coordinates and a basis set contracted using a diagonalization and truncation procedure to calculate the energy levels of H_3^+ . This procedure produced results broadly in agreement with Tennyson and Henderson (1989) but extending to about 25 000 cm^{-1} above the vibrational ground state. They noted, as have other workers, that this is actually the limit of validity of the MBB potential. However, as the potential remains well behaved up to the dissociation limit of H_3^+ at about 35 000 cm^{-1} , it has widely been used up to this energy even though the actual dissociation limit given by the potential is somewhat higher than this.

Some workers have checked results with the less accurate DIM potential (Preston and Tully 1971) which behaves qualitatively correctly for all H_3^+ geometries without finding any significant differences in behaviour between the two potentials. In general, classical calculations on the DIM potential show that rather more of the phase space is filled with chaotic trajectories than with the MBB potential; quantal comparisons similarly show wavefunctions obtained using the DIM to be more irregular.

Henderson and Tennyson (1990) adapted their previous calculations to a DVR in all three vibrational coordinates. This enabled them to obtain estimates of the energy level of *all* bound vibrational states of H_3^+ ; they found 881 vibrational states for the MBB potential

lying $35\,000\text{ cm}^{-1}$ or less above the vibrational ground state. Furthermore Henderson and Tennyson found that many of their states lay significantly below those of Carter and Meyer (1990).

Carter and Meyer (1992) criticized Henderson and Tennyson's (1990) calculations as being non-variational and suggested that this problem was due to use of incorrect boundary conditions at linear geometries. A preliminary analysis by Henderson *et al* (1992) confirmed the non-variational behaviour but suggested that the problem was not due to boundary conditions. A more detailed study (Henderson *et al* 1993) showed that the problem was due to a failure of what is usually called the quadrature approximation (Dickinson and Certain 1968) in their DVR.

Henderson *et al* (1993) recomputed their previous 3D DVR results to a much tighter convergence limit of $\sim 2\text{ cm}^{-1}$ at $35\,000\text{ cm}^{-1}$. This new calculation removed the largest disagreement with the results of Carter and Meyer (1990, 1992), but Henderson *et al* still obtained results for non- A_1 symmetries lower than the convergence limits claimed by Carter and Meyer. The source of this discrepancy was only revealed when Bramley *et al* (1993) discovered that there were two subtly different versions of the MBB potential in common use! Naturally Carter and Meyer had been using the correct, if less commonly used, version of this potential which has been used in all subsequent calculations.

Recently Bramley *et al* (1994) solved the H_3^+ problem on the MBB potential using a huge, uncontracted DVR basis in scattering coordinates. They did this by taking advantage of the sparseness of the Hamiltonian matrix in the uncontracted DVR. Their method was based on iterative diagonalization with non-zero matrix elements calculated as they were required (Bramley and Carrington 1993). Although their method can give wavefunctions, at considerable extra computational cost, only energy levels were obtained. Bramley *et al*'s results were outstandingly accurate yielding energy levels converged to 0.01 cm^{-1} or about 3 parts in 10^7 at the dissociation limit. Their results broadly confirmed the recalculations of Henderson *et al* (1993) although they showed that Henderson *et al*'s convergence claims for the highest few levels were somewhat optimistic.

There are two other calculations on the high-lying vibrational levels of H_3^+ that should be mentioned. These are by Day and Truhlar (1991) and Bačić and Zhang (1991), and employed a very similar technique. These authors noted the success of the Jacobi or scattering coordinates in various calculations on H_3^+ but these coordinates suffered from the defect of not possessing the correct symmetry for the molecule. They therefore developed (contracted) basis functions in all three possible sets of Jacobi coordinates simultaneously. These functions could then be symmetrized correctly for the molecule but suffered from the problem that the basis set was now non-orthogonal as well as potentially overcomplete and hence linearly dependent. This method was of interest not only because of the intrinsic importance of results on the H_3^+ system, but also because similar combinations of coordinates are routinely used for reactive scattering calculations and these bound-state calculations gave an opportunity of testing the methodology against other procedures.

Day and Truhlar's (1991) and Bačić and Zhang's (1991) calculations gave broadly similar results obtaining well converged energy levels in a similar range, up to $\sim 25\,000\text{ cm}^{-1}$, covered by Carter and Meyer (1990). The main difference between the two calculations was their approach to spurious levels which occurred as a result of linear dependence in their basis sets. Day and Truhlar (1991) simply stopped their calculation at their last non-linearly dependent level, while Bačić and Zhang's (1991) identified the offending levels, removed them from their calculation and carried on.

12.3. Rotational states at dissociation

Although explanations of the Carrington–Kennedy spectrum require a centrifugal barrier and hence rotationally excited states, there has been significantly less work on high-lying rotational states of H_3^+ than on the equivalent vibrational states. As mentioned above Miller and Tennyson (1988a) exploited the two-step procedure of Tennyson and Sutcliffe (1986) to find the highest rotational angular momentum which supported a truly bound state. They performed these calculations on both H_3^+ and H_2D^+ , and a variety of potential energy surfaces. Their results were generally in line with the classical predictions of Berblinger *et al* (1988a, 1989).

Solving the near dissociation problem for rotationally excited states with intermediate J is a much more challenging problem as the number of states involved is potentially enormous. Tennyson and Henderson (1989) presented results for the $J = 1$ levels associated with the first 41 vibrational states of H_3^+ , as part of their 1D DVR study of the $J = 0$ problem. This range extended well above the barrier to linearity. However, as noted by themselves and Bačić and Zhang (1992), their results were poorly converged.

Bačić and Zhang (1992) adapted their method based on the use of three sets of Jacobi coordinates to rotationally excited problems. They computed $J = 1$ levels up to the 18 000–24 000 cm^{-1} region, depending on symmetry. Tennyson (1993) developed a two-step rotational procedure based on using 3D DVR vibrational wavefunctions for which the angular coordinate is transformed back to a basis set representation for inclusion of the Coriolis coupling term. He gave results for $J = 1$ up to the 21 000–24 000 cm^{-1} region, again depending on the symmetry of the state. Tennyson found good agreement with the previous calculations of Bačić and Zhang, but noted that both calculations appeared to give better convergence for some symmetry blocks than others. Not surprisingly, given the different procedures employed, this differential convergence varied between the calculations.

Recently Carter and Meyer (1994) have used their hyperspherical coordinates based method to give results for both $J = 1$ and $J = 2$ into the region studied by Bačić and Zhang (1992) and Tennyson (1993). They note good agreement with the $J = 1$ results of Bačić and Zhang. Carter and Meyer also present results for higher J states which lie below barrier extending the previous MBB calculations of Miller and Tennyson (1988c, 1989). However, since Carter and Meyer's method does not use any intermediate separation between vibrational and rotational motion it would appear to be more difficult to extend to very high levels of excitation efficiently.

In still unpublished results Henderson and Tennyson (1995) have used the method of Tennyson (1993) to compute rotationally excited states of the H_3^+ all the way to dissociation for $J = 1$ and $J = 2$. These calculations were computationally expensive, taking several days on a Convex 3480 computer, and have yet to be fully analysed. However, comparison with classical density-of-state calculations, see figure 12, suggest that these calculations are indeed converged.

The calculation of all the rotational levels up to dissociation is a significant step forward as it lays open, for the first time, the possibility of calculating fully quantal spectra of H_3^+ in the dissociation region. A DVR based dipole transition intensity program, DIPOLE3, has been written which can calculate the appropriate transition intensities efficiently (Lynas Gray *et al* 1995, Tennyson *et al* 1995) and hopefully this next significant step will not be long delayed.

12.4. Of horseshoes and elephants' feet

There has been a substantial amount of work performed on perfecting quantum mechanical methods for treating the near dissociation region. Much of this work has been

developmental, but some analysis of results has been performed in the context of the Carrington–Kennedy spectrum. In particular, it should be noted that the calculations of Henderson and Tennyson (1990) and Henderson *et al* (1993) yielded not only energy levels but also wavefunctions.

Analysis of wavefunction plots from a number of calculations (Gomez Llorente *et al* 1988, 1989, Tennyson and Henderson 1989, Tennyson *et al* 1990a, Brass *et al* 1990, Henderson and Tennyson 1990, Polieveja *et al* 1994b) show wavefunctions with a build up of amplitude in the region of the horseshoe periodic orbit, see figure 13. This behaviour, known as scarring, is expected to be the consequence of any underlying regular classical motion (McDonald and Kaufman 1979, Heller 1984).

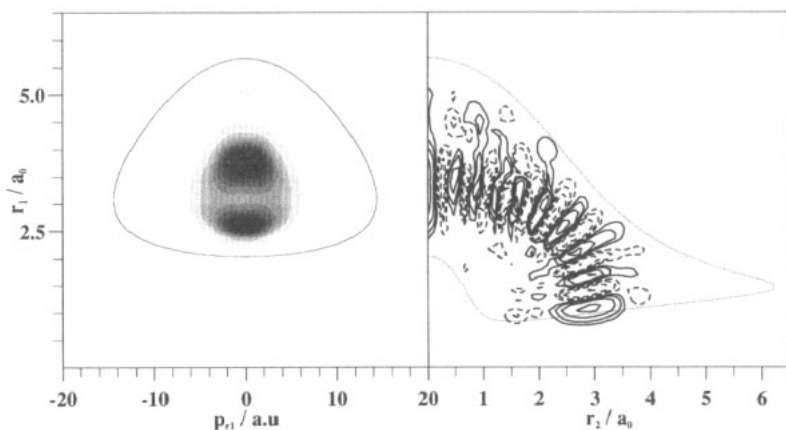


Figure 13. Right: wavefunction for an H_3^+ horseshoe state plotted in scattering coordinates, r_1 against r_2 with $\theta = 90^\circ$ fixed. Positive and negative amplitudes are indicated with the full and broken contours respectively; the faint line indicates the classical turning point for this state. Left: Husimi plot of the wavefunction shown on the right, plotted for r_1 against p_{r_1} . Fixed coordinates are $\theta = 90^\circ$, $p_\theta = 0$, $r_2 = 10^{-5}a_0$ and p_{r_2} obtained from the energy. Darker regions in the plot indicate higher amplitudes. Adapted from Polavieja *et al* (1994b).

Classically the ‘normal mode’ periodic orbits of the low-lying bending motion and the horseshoe periodic orbit are different motions (Pollak 1989). However, Henderson and Tennyson (1990) found that they could identify wavefunctions corresponding to a single series of bending states starting from the bending fundamental, ν_2 , and extending in a single progression all the way to a state they labelled $19\nu_2$ which lay just above the dissociation limit of the MBB potential. They commented that the horseshoe states are perhaps better thought of as highly excited bending states of a quasilinear molecule.

Le Sueur *et al* (1993) used the wavefunctions of Henderson *et al* (1993) to compute vibrational band intensities for the H_3^+ system. As rotationless vibrational band intensities can only be approximate and this approximation is really only valid for small amplitude motion (Le Sueur *et al* 1992), they chose to analyse transitions from the vibrational ground state and other low-lying levels to all the other bound vibrational states. These calculations show strong, periodic structures in the strength of the transitions. Analysis shows that the peak of each structure corresponds to a horseshoe state but in each case several other nearby states are also significantly brightened, presumably by intensity stealing from the horseshoe. Le Sueur *et al*’s results suggest (Hamilton 1993) that H_3^+ should have a clearly

observable rotation–vibration spectrum in the optical, but no such experiment has as yet been performed.

Recently Polavieja *et al* (1994b) have used phase-space-based ideas to analyse H_3^+ vibrational wavefunctions. Phase space is an implicitly classical concept, however two distributions due to Wigner (1932) and Husimi (1940), have been proposed which allow the transformation of wavefunctions into ‘quantum phase space’. The Husimi distribution, in contrast to Wigner’s, obeys the uncertainty principle and therefore shows little detailed structure. It is also, as a consequence, considerably cheaper to calculate from a given wavefunction.

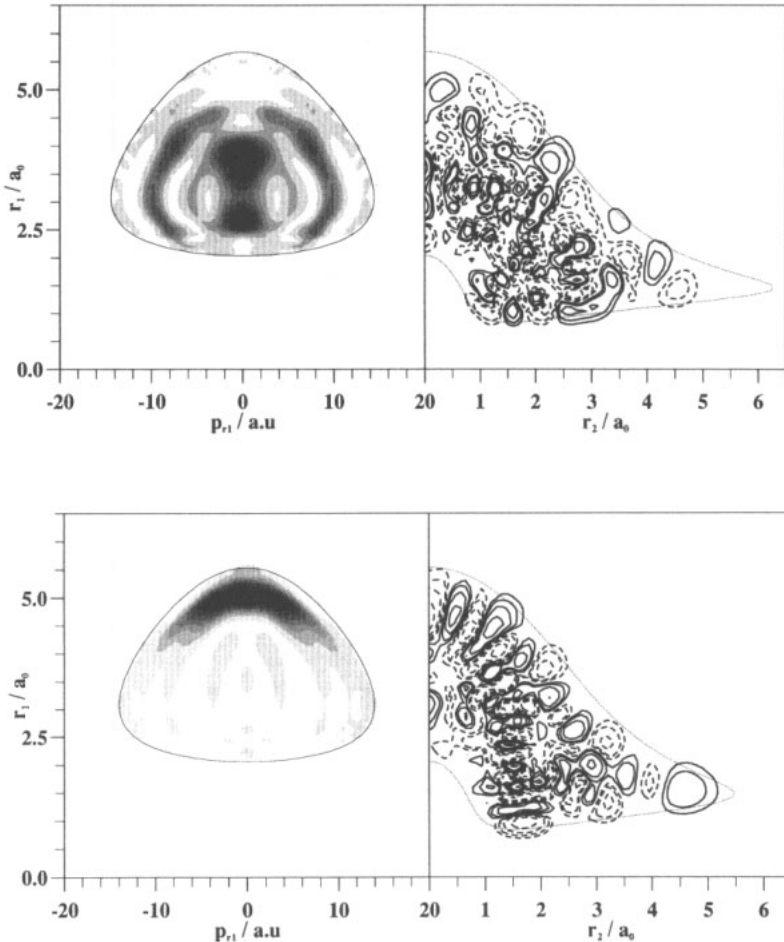


Figure 14. Top right: wavefunction for an H_3^+ state showing scarring along the elephant’s foot motion. Top left: Husimi plot of the wavefunction shown top right. Bottom right: Band wavefunction obtained from an envelope of states centred on the wavefunction shown top right. Bottom left: Husimi plot of the bottom right wavefunction. Other details are as in figure 13. Adapted from Polavieja *et al* (1994b) and Fulton (1994).

Polavieja *et al* (1994b) analysed Henderson *et al*’s (1993) wavefunctions using Husimi distributions. They found, besides strong localization about the horseshoe periodic orbit (figure 13), a number of other features some of which had been previously overlooked.

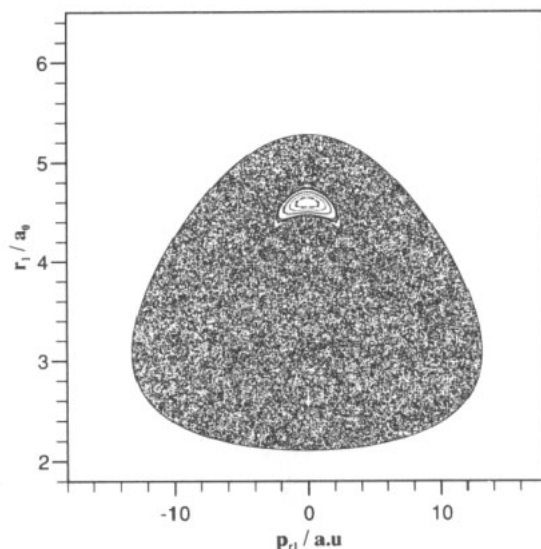


Figure 15. Poincaré surface of section for trajectories in the (r_1, r_2) coordinates with θ fixed at 90° . The cut is for r_1 against its conjugate momentum for a near linear geometry, i.e. $r_2 \sim 0$. The outer curve gives edge of the allowed phase space at this energy. The dominant regular structure is due to the horseshoe periodic orbit. The dots are due to chaotic trajectories. The small blank region in the lower middle of the figure is where the elephant's foot periodic orbit was found. The figure is from Fulton (1994).

Of particular interest was a feature shown in figure 14 which corresponds to another motion where one H atom passed between the others but on a somewhat broader trajectory. This motion has jokingly been labelled the elephant's foot and is found to be particularly prominent in the dissociation region. Having identified the scarring of the wavefunction due to this feature, the classical orbit was also readily identified, see figure 11.

It is not surprising that the quasiperiodic orbit was overlooked in previous classical studies as it occupies a very small volume in phase space. Figure 15 shows a Poincaré surface of section for T-shaped H_3^+ . The cut is near the linear geometries and the prominent regular features (invariant tori) are due to the horseshoe motion. The elephant's foot causes the small spot in the lower middle of the figure in which no trajectories are observed. To find invariant tori due to the elephant's foot it is necessary to inspect this small region in detail (Fulton 1994).

Neither the horseshoe nor elephant's foot periodic orbits are an artifact of single potential energy surfaces. Polavieja *et al* (1994b) found them on the MBB and DIM potentials and a surface constructed from three Morse oscillators.

Polavieja *et al* (1994a) developed a method finding and highlighting underlying regular features which may be hidden because they are spread across several wavefunctions. This method involves constructing wavepackets at maxima in a Husimi distribution and then convoluting the wavefunctions which contribute strongly to this wavepacket. The resulting wavefunction, which is no longer a stationary state, can be called a band wavefunction.

Polavieja *et al* (1994b) used this method to study the H_3^+ wavefunctions of Henderson *et al* (1993). As demonstrated in figure 14, the resulting band wavefunctions make the underlying motion much more clearly visible in what are otherwise rather noisy

wavefunctions. The availability of full sets of quantal wavefunctions combined with the ability to view these in a number of different ways (see for example Sadovskii *et al* 1993) has opened up a number of new possibilities for this line of research (Fulton 1994).

13. Conclusions

The electronic simplicity of H_3^+ is beguiling; it hides the tremendous richness of the nuclear dynamics of the system. This richness manifests itself in the unusual spectroscopy both in the conventional spectroscopic domain of the low-lying states of the system and the behaviour of the system near-dissociation. The study of these problems touches physics, chemistry and astronomy and combines observation with *ab initio* quantum mechanics.

Since the first spectrum of H_3^+ was observed in 1980, a tremendous amount of ground has been covered in a relatively short time. There are, however, a number of milestones which are still to be passed. The observation of H_3^+ in the interstellar medium is an important one; as is the full quantum mechanical elucidation of the near dissociation spectrum recorded by Carrington and co-workers. A host of other problems concerning such things as dissociative recombination, the pure rotational spectrum and the *infrared* spectrum of the metastable $^3\Sigma_u^+$ state remain to be solved. These are obvious targets. It would seem almost certain that H_3^+ will throw up a few more surprises before its story is fully told.

Acknowledgments

I would like to state my gratitude to the subject of this review. The H_3^+ ion has opened doors for me that I never guessed would be opened; doors that led to new scientific opportunities and unexpected public exposure, and doors which led me to interesting places and new friendships. I must also thank Steven Miller for many helpful discussions during the course of my writing this review, Nic Fulton and James Henderson for providing figures and Iain McNab for sending me an advanced copy of his own review and other information. Finally Bianca Dinelli, Iain McNab, Steven Miller, T Oka, Oleg Polyansky and J K G Watson provided very helpful comments on my draft manuscript.

References

- Adams N G and Smith D 1987 *Astrochemistry IAU Symp. 120* ed M S Vardya and S P Tarafdar (Reidel: Dordrecht) p 1
 — 1988 *Rate Coefficients in Astrochemistry* ed T J Millar and D A Williams (Kluwer: Dordrecht) pp 173–92
 — 1989 *Dissociative Recombination: Theory, Experiment and Applications* ed J B A Mitchell and S L Guberman (World Scientific: Singapore) p 124
 Ahlrichs R, Votava C and Zirz C 1977 *J. Chem. Phys.* **66** 2771–2
 Amano T 1985 *J. Opt. Soc. Am. B* **2** 790–3
 — 1988 *Astrophys. J.* **329** L121–4
 — 1990 *J. Chem. Phys.* **92** 6492–501
 Amano T and Watson J K G 1984 *J. Chem. Phys.* **91** 2869–71
 Amano T, Chan M-C, Civis S, McKellar A R W, Majewski W A, Sadovskii D and Watson J K G 1994 *Can. J. Phys.* **72**
 Anderson J B 1992 *J. Chem. Phys.* **96** 3702–6
 Angerhofer P, Churchwell E and Porter R N 1978 *Astrophys. Lett.* **19** 137
 Atreya S K and Donahue T M 1976 *Jupiter* ed T Gehrels (Tucson, AZ: University of Arizona Press) p 304
 Bačić Z and Light J C 1989 *Ann. Rev. Phys. Chem.* **40** 469–98

- Bačić Z and Zhang J Z H 1991 *Chem. Phys. Lett.* **184** 513–20
— 1992 *J. Chem. Phys.* **98** 3707–13
- Bae Y K and Cosby P C 1990 *Phys. Rev. A* **41** 1741–3
- Ballester G E, Miller S, Tennyson J, Trafton L M and Geballe T R 1994 *Icarus* **107** 189–94
- Bardo R D and Wolfsberg M 1978 *J. Chem. Phys.* **68** 2686–95
- Baron R, Joseph R D, Owen T, Tennyson J, Miller S and Ballester G E 1991 *Nature* **353** 539–42
- Bartlett P and Howard B J 1990 *Mol. Phys.* **70** 1001–29
- Bates D R 1950 *Phys. Rev.* **78** 492–3
— 1993 *Proc. R. Soc. A* **443** 257–64
- Bates D R, Guest M F and Kendall R A 1993 *Planet. Space Sci.* **41** 9–15
- Bawendi M G, Rehffuss B D and Oka 1990 *J. Chem. Phys.* **93** 6200–9
- Berblinger M and Schlier C 1988 *Mol. Phys.* **63** 779–90
— 1992 *J. Chem. Phys.* **96** 6834–41
— 1993 Private communication
— 1994 *J. Chem. Phys.* **101** 4750–8
- Berblinger M, Gomez-Llorrente J M, Pollak E and Schlier C 1988a *Chem. Phys. Lett.* **146** 353–7
Berblinger M, Pollak E and Schlier C 1988b *J. Chem. Phys.* **88** 5643–56
- Berblinger M, Schlier C and Pollak E 1989 *J. Chem. Phys.* **93** 2319–28
- Berblinger M, Schlier C, Tennyson J and Miller S 1992 *J. Chem. Phys.* **96** 6842–49
- Black J H 1993 *J. Chem. Soc. Faraday Trans.* **89** 2171
- Black J H, Van Dishoeck E F, Willner S P and Woods R C 1990 *Astrophys. J.* **358** 459–67
- Bogey M, Demuyneck C, Denis M, Destombes J L and Lemoine 1984 *Astron. Astrophys.* **137** L15–6
- Boreiko R T and Betz A L 1993 *Astrophys. J.* **405** L39–42
- Bramley M J and Carrington T Jr 1993 *J. Chem. Phys.* **99** 8519–41
- Bramley M J, Henderson J R, Tennyson J and Sutcliffe B T 1993 *J. Chem. Phys.* **98** 10104–5
- Bramley M J, Tromp J W, Carrington T Jr and Corey G C 1994 *J. Chem. Phys.* **100** 6175–94
- Brass O, Tennyson J and Pollak E 1990 *J. Chem. Phys.* **92** 3377–86
- Broadfoot A L *et al* 1986 *Science* **233** 74–9
- Brown R D and Rice E H N 1986 *Mon. Not. R. Astron. Soc.* **223** 429–42
- Bunker P R 1979 *Molecular Symmetry and Spectroscopy* (New York: Academic)
- Burton P G, Von Nagy-Felsobuki E and Doherty G 1984 *Chem. Phys. Lett.* **104** 323–30
- Canosa A, Gomet J C, Rowe B R, Mitchell J B A and Queffelec J L 1992 *J. Chem. Phys.* **97** 1028–37
- Carney G D 1980 *Chem. Phys.* **54** 103–7
- Carney G D and Porter R N 1974 *J. Chem. Phys.* **60** 4251–64
— 1976 *J. Chem. Phys.* **65** 3547–65
— 1977 *Chem. Phys. Lett.* **50** 327–9
— 1980 *Phys. Rev. Lett.* **45** 537–41
- Carney G D, Sprandel L L and Kern C W 1978 *Adv. Chem. Phys.* **37** 305–79
- Carrington A and Kennedy R A 1984 *J. Chem. Phys.* **81** 91–112
- Carrington A and McNab I R 1989 *Acc. Chem. Res.* **22** 218–22
- Carrington A, Buttenshaw J and Kennedy R A 1982 *Mol. Phys.* **45** 753–8
- Carrington A, McNab I R and West Y D 1993 *J. Chem. Phys.* **98** 1073–92
- Carter S and Meyer W 1990 *J. Chem. Phys.* **93** 8902–14
— 1992 *J. Chem. Phys.* **96** 2424–5
— 1994 *J. Chem. Phys.* **100** 2104–17
- Chambers A V and Child M S 1988 *Mol. Phys.* **65** 1337–44
- Chen C-L, Maessen B and Wolfsberg M 1985 *J. Chem. Phys.* **83** 1795–807
- Child M S 1986a *J. Chem. Soc., Faraday Trans.* **2** **82** 1143–9
— 1986b *J. Phys. Chem.* **90** 3595–9
— 1991 *Semiclassical Mechanics with Molecular Applications* (Oxford: Clarendon)
- Christoffersen R E 1964 *J. Chem. Phys.* **41** 960–71
- Connerney J E P, Baron R, Satoh T and Owen T 1993 *Science* **262** 1035–8
- Cosby P C and Helm H 1988 *Chem. Phys. Lett.* **152** 71–4
- Dalgarno A 1994 *Adv. At. Mol. Opt. Phys.* **32** 57–68
- Dalgarno A, Oppenheimer M and Berry R S 1973 *Astrophys. J.* **183** L21–4
- Day P N and Truhlar D G 1991 *J. Chem. Phys.* **95** 6615–21
- Dempster A J 1916 *Phil. Mag.* **31** 438–43
- Dickinson A S and Certain P R 1968 *J. Chem. Phys.* **49** 4209–11
- Dinelli B M, Miller S and Tennyson J 1992 *J. Mol. Spectrosc.* **153** 718–25

- 1994 *J. Mol. Spectrosc.* **163** 71–9
- Dinelli B M, Le Sueur C R, Tennyson J and Amos R D 1995 *Chem. Phys. Lett.* **232** 295–300
- Dinelli B M, Miller S, Achilleos N, Lam H A, Tennyson J, Jagod M-F, Oka T, Geballe T R, Brooke T, Ballester G E and Trafton L M 1994b *Bull. Am. Astron. Soc.* **26** 02.22-p
- Drolshagen G, Gianturco F A and Toennies J P 1989 *Israel J. Chem.* **29** 417–25
- Drossart P *et al* 1989 *Nature* **340** 539–41
- Drossart P, Maillard J-P, Caldwell J and Rosenqvist J 1993 *Astrophys. J.* **402** L25–8
- Figger H, Ketterle W and Walther H 1989 *Z. Phys. D* **13** 129–37
- Flower D R 1989 *J. Phys. B: At. Mol. Opt. Phys.* **22** 2319–39
- Foster S C, McKellar A R W, Peterkin I R, Watson J K G, Pan F S, Crofton M W, Altman R S and Oka T 1986a *J. Chem. Phys.* **84** 91–9
- Foster S C, McKellar A R W and Watson J K G 1986b *J. Chem. Phys.* **85** 664–70
- Fulton N G 1994 *PhD Thesis* University of London
- Gaillard M J, Gemmell D S, Goldring G, Levine I, Pietsch W J, Poizat J C, Ratkowski A J, Remillieux J, Vager Z and Zabransky B J 1978 *Phys. Rev. A* **17** 1797–803
- Geballe T R 1993 Private communication
- Geballe T R and Oka T 1989 *Astrophys. J.* **342** 855–9
- Geballe T R, Jagod M-F and Oka T 1993 *Astrophys. J.* **408** L109–12
- 1994 Private communication
- Genzel R and Stutzki J 1989 *Ann. Rev. Astron. Astrophys.* **27** 41–85
- Gerard J C, Dols V, Paresce F and Prangé R 1993 *J. Geophys. Res. Planets* **98** 18973–80
- Gerlich D 1993 *J. Chem. Soc. Faraday Trans* **89** 2167 and 2168
- Gomez Llorente J M and Pollak E 1987 *Chem. Phys. Lett.* **138** 125–30
- 1988 *Chem. Phys.* **120** 37–49
- 1989 *J. Chem. Phys.* **90** 5406–19
- Gomez Llorente J M, Zakrzewski J, Taylor H S and Kulander K C 1988 *J. Chem. Phys.* **89** 5959–60
- 1989 *J. Chem. Phys.* **90** 1505–18
- Guberman S L 1994 *Phys. Rev. A* **49** R4277–9
- Hamilton D C, Gloeckler G, Krimigis S M, Bostrom C O, Armstrong T P, Ashford W I, Fan C Y, Lagerotti L J and Hunte D M 1980 *Geophys. Res. Lett.* **7** 813–6
- Hamilton P A 1993 Private communication
- Handy N C, Yamaguchi Y and Schaefer H F III 1986 *J. Chem. Phys.* **84** 4481–4
- Harris D O, Engerholm G O and Gwinn W 1965 *J. Chem. Phys.* **43** 1515–7
- Heller E J 1984 *Phys. Rev. Lett.* **53** 1515–8
- Henderson J R and Tennyson J 1990 *Chem. Phys. Lett.* **173** 133–8
- 1995 to be published
- Henderson J R, Tennyson J and Sutcliffe B T 1992 *J. Chem. Phys.* **96** 2426–7
- 1993 *J. Chem. Phys.* **98** 7191–203
- Herbst E 1982 *Astron. Astrophys.* **111** 76–80
- Herbst E and Klempner W 1973 *Astrophys. J.* **185** 505–33
- Herzberg G 1967 *Trans. R. Soc. Canada* **5** 3
- 1987 *Ann. Rev. Phys. Chem.* **38** 27–56
- 1990a *Spectrochim. Acta A* **89** 63–74
- 1990b *J. Mol. Spectrosc.* **217** 11–8
- Hibbins R E, Miles J R and Sarre P J 1994 *Molecules and Grains in Space (AIP Conf. Proc. 312)* ed I Nenner (New York: APS) pp 87–97
- Hirschfelder J O 1938 *J. Chem. Phys.* **6** 795–806
- Hirschfelder J O and Weygandt O N 1938 *J. Chem. Phys.* **6** 806–10
- Husimi K 1940 *Proc. Phys. Math. Soc. Japan* **22** 264–314
- Hutson J M 1990 *Ann. Rev. Phys. Chem.* **41** 123–54
- Iida M, Ohshima Y and Endo Y 1991 *Astrophys. J.* **371** L45–6
- Jennings D A, Demuyneck C, Banek M and Evenson K M 1990 quoted by Polyansky and McKellar (1990) and private communication
- Jensen P 1989 *J. Mol. Spectrosc.* **133** 438–60
- Jensen P and Špirko V 1986 *J. Mol. Spectrosc.* **118** 208–31
- Jensen P, Špirko V and Bunker P R 1986 *J. Mol. Spectrosc.* **115** 269–93
- Kao L, Oka T, Miller S and Tennyson J 1991 *Astrophys. J. Suppl.* **77** 317–29
- Ketterle W, Messner H-P and Walther H 1989a *Europhys. Lett.* **8** 333–8
- Ketterle W, Figger H and Walther H 1989b *Z. Phys. D* **13** 139–46

- Kim S, Drossart P, Caldwell J and Maillard J-P 1990 *Icarus* **84** 54–61
- Kim S J, Drossart P, Caldwell J, Maillard J-P, Herbst T and Shure M 1991 *Nature* **353** 536–9
- Kim Y H, Fox J L and Porter H S 1992 *J. Geophys. Res.* **97** 6093–101
- Kolos W and Wolniewicz L 1965 *J. Chem. Phys.* **43** 2429–41
- Kozin I N, Polyansky O L and Zobov N F 1988 *J. Mol. Spectrosc.* **128** 126–34
- Krimigis S M and Roelof E C 1983 *Physics of the Jovian Magnetosphere* ed A J Dressler (Cambridge: Cambridge University Press) p 106
- Kulander K C and Guest M F 1979 *J. Phys. B: At. Mol. Phys.* **12** L501–4
- Lam H A, Miller S, Joseph R D and Tennyson J 1994 *Astrophys. J. Lett.* submitted
- Larsson M *et al* 1993 *Phys. Rev. Lett.* **70** 430–3
- Lee S S, Ventrudo B F, Cassidy D T, Oka T, Miller S and Tennyson J 1991 *J. Mol. Spectrosc.* **145** 222–4
- Lembo L J, Petit A and Helm H 1989 *Phys. Rev. A* **39** 3721–4
- Lequeux J and Roueff E 1991 *Phys. Rep.* **200** 241–99
- Le Sueur C R, Miller S, Tennyson J and Sutcliffe B T 1992 *Mol. Phys.* **76** 1147–56
- Le Sueur C R, Henderson J R and Tennyson J 1993 *Chem. Phys. Lett.* **206** 429–36
- Lie G C and Frye D 1992 *J. Chem. Phys.* **96** 6784–90
- Lubic K G and Amano T 1984 *Can. J. Phys.* **62** 1886–8
- Lucy L B, Danziger I J and Gouiffes C 1991 *Astron. Astrophys.* **243** 223–9
- Lynas Gray A'E, Miller S and Tennyson J 1995 *J. Mol. Spectrosc.* **169** 6458
- Macdonald J A, Biondi M A and Johnsen R 1984 *Planet. Space Sci.* **32** 651–4
- Maillard J-P, Drossart P, Watson J K G, Kim S J and Caldwell J 1990 *Astrophys. J.* **363** L37–41
- Majewski W A, Marshall M D, McKellar A R W, Johns J W C and Watson J K G, 1987 *J. Mol. Spectrosc.* **122** 341–55
- Majewski W A, Feldman P A, Watson J K G, Miller S and Tennyson J 1989 *Astrophys. J.* **347** L51–4
- Majewski W A, McKellar A R W, Sadovskii D and J K G Watson 1994 *Can. J. Phys.* **72** 1016
- Marten A, Debergh C, Owen T, Gautier D, Maillard J-P, Drossart P, Lutz B L, Orton G S 1994 *Planet. Space Sci.* **42** 391–9
- McDonald S W and Kaufman A N 1979 *Phys. Rev. Lett.* **42** 1189–91
- McNab I R 1995 *Adv. Chem. Phys.* **89** 1–87
- McWeeny R 1989 *Methods of Molecular Quantum Mechanics* 2nd edn (London: Academic)
- Meikle W P S, Allen D A, Spyromilio J and Varani G-F 1989 *Mon. Not. R. Astron. Soc.* **238** 193–223
- Meyer W, Botschwina P and Burton P G 1986 *J. Chem. Phys.* **84** 891–900
- Michels H H and Hobbs R H 1984 *Astrophys. J.* **286** L27–9
- Millar T J, Bennet A and Herbst E 1989 *Astrophys. J.* **340** 906–20
- Miller S and Tennyson J 1987 *J. Mol. Spectrosc.* **128** 183–92
- 1988a *Chem. Phys. Lett.* **145** 117–20
- 1988b *Astrophys. J.* **335** 486–90
- 1988c *J. Mol. Spectrosc.* **128** 530–9
- 1989 *J. Mol. Spectrosc.* **136** 223–40
- 1992 *Chem. Soc. Reviews* **21** 281–8
- Müller S, Tennyson J and Sutcliffe B T 1989 *Mol. Phys.* **66** 429–56
- 1990a *J. Mol. Spectrosc.* **141** 104–117
- Miller S, Joseph R D and Tennyson J 1990b *Astrophys. J.* **360** L55–8
- Miller S, Tennyson J, Lepp S and Dalgarno A 1992 *Nature* **355** 420–2
- Miller S, Lam H A and Tennyson J 1994 *Can. J. Phys.* **72** 760
- Miller S *et al* 1995 *Geophys. Res. Lett.* in press
- Morrison D and Samz J 1980 *Voyage to Jupiter* (Washington: NASA)
- Murrell J N and Bosanac S D 1989 *Introduction to the Theory of Atomic and Molecular Collisions* (Chichester: Wiley) ch 5.5
- Murrell J N, Carter S, Farantos S C, Huxley P and Varandas A J C 1984 *Molecular Potential Energy Functions* (Chichester: Wiley) ch 11
- Nakanaga T, Ito F, Sugawara K, Takeo H and Matsumura C 1990 *Chem. Phys. Lett.* **169** 269–73
- Oka T 1980 *Phys. Rev. Lett.* **45** 531–4
- 1981 *Phil. Trans. R. Soc. A* **303** 543–9
- 1983 *Molecular Ions: Spectroscopy, Structure and Chemistry* ed T A Miller and V E Bondybey (Amsterdam: North-Holland) pp 73–90
- 1992a *Rev. Mod. Phys.* **64** 1141–9
- 1992b *Proc. Int. School of Physics 'Enrico Fermi'* ed T W Häusch (Amsterdam: North-Holland) pp 61–87
- 1993 *J. Chem. Soc. Faraday Trans.* **89** 2171

- Oka T and Geballe T R 1990 *Astrophys. J.* **351** L53–6
- Oka T and Jagod M-F 1993 *J. Chem. Soc. Faraday Trans* **89** 2147–54
- Orton G S *et al* 1995 *Science* in press
- Pagini L, Wannier P G, Frerking M A, Kuiper T B H, Gulkis S, Zimmerman P, Encrenaz P J, Whiteoak J B, Destombes J L and Pickett H M 1992a *Astron. Astrophys.* **258** 472–78
- Pagini L, Salez M and Wannier P G 1992b *Astron. Astrophys.* **258** 479–88
- Pan F-S and Oka T 1986 *Astrophys. J.* **305** 518–25
- Pfeiffer R and Child M S 1987 *Mol. Phys.* **60** 1367–78
- Phillips T G, Blake G A, Keene J, Woods R C and Churchwell E 1985 *Astrophys. J.* **294** L45–8
- Pineau des Forets G, Roueff E and Flower D R 1992 *Mon. Not. R. Astron. Soc.* **258** 45–7
- Polavieja G G, Borondo F and Benito R M 1994a *Phys. Rev. Lett.* **73** 1613–6
- Polavieja G G, Fulton N G and Tennyson J 1994b *Mol. Phys.* **83** 361–79
- Pollak E 1987 *J. Chem. Phys.* **86** 1645–6
- 1989 Private communication
- Pollak E and Schlier C 1989 *Acc. Chem. Res.* **22** 223–9
- Polyansky O L 1985 *J. Mol. Spectrosc.* **112** 79–87
- Polyansky O L and McKellar A R W 1990 *J. Chem. Phys.* **92** 4039–43
- Polyansky O L, Miller S and Tennyson J 1993 *J. Mol. Spectrosc.* **157** 237–47
- Polyansky O L, Dinelli B M, Le Sueur C R and Tennyson J 1995a *J. Chem. Phys.* submitted
- Polyansky O L, Dinelli B M and Tennyson J 1995b to be published
- Prangé R 1991 *Astron. Astrophys.* **251** L15–8
- Preisikorn A, Frye D and Clementi E 1991 *J. Chem. Phys.* **94** 7204–7
- Preston R K and Tully J C 1971 *J. Chem. Phys.* **54** 4297–304
- Quack M 1977 *Mol. Phys.* **34** 477–504
- 1990 *Phil. Trans. R. Soc. A* **332** 203–20
- Röhse R, Klopper W and Kutzelnigg W 1993 *J. Chem. Phys.* **99** 8830–9
- Röhse R, Klopper W, Kutzelnigg W and Jaquet R 1994 *J. Chem. Phys.* **101** 2231–43
- Sadovskii D A, Fulton N G, Henderson J R, Tennyson J and Zhilinskii B I 1993 *J. Chem. Phys.* **99** 906–18
- Saito S, Kawaguchi K and Hirota E 1985 *J. Chem. Phys.* **82** 45–7
- Sarpal B K, Tennyson J and Morgan L A 1994 *J. Phys. B: At. Mol. Opt. Phys.* **27** 5943–53
- Schaad L J and Hicks W V 1974 *J. Chem. Phys.* **72** 3909–15
- Schild H, Miller S and Tennyson J 1994 unpublished work
- Schinke R, Dupuis M and Lester W A Jr 1980 *J. Chem. Phys.* **72** 3909–15
- Schlier C and Vix U 1985 *Chem. Phys.* **95** 401–9
- Schutte W A, Tielens A G G M, Allamandola L J, Cohen M and Wooden D H 1990 *Astrophys. J.* **360** 577–89
- Shy J-T, Farley J W, Lamb W E Jr and Wing W H 1980 *Phys. Rev. Lett.* **45** 535–7
- Shy J-T, Farley J W and Wing W H 1981 *Phys. Rev. A* **24** 1146–9
- Sidhu K S, Miller S and Tennyson J 1992 *Astron. Astrophys.* **255** 453–6
- Smith D and Spanel P 1993 *Chem. Phys. Lett.* **211** 454–60
- Smith D, Adams N G and Alge E 1982 *Astrophys. J.* **263** 123–9
- Špirko V, Jensen P, Bunker P R and Cejchan A 1985 *J. Mol. Spectrosc.* **112** 183–202
- Steinmetzger U, Redpath A and Ding A 1982 *Ber. Bunes. Phys. Chem.* **86** 468
- Sundstrom G *et al* 1994 *Science* **263** 785–7
- Sutcliffe B T 1980 *Quantum Dynamics of Molecules* ed R G Woolley (New York: Plenum) p 1
- 1982 *Current Aspects of Quantum Chemistry (Studies in Theoretical Chemistry 21)* ed R Carbo (Amsterdam: Elsevier) pp 99–125
- 1992 *Mol. Phys.* **75** 1233–36
- Sutcliffe B T and Tennyson J 1991 *Int. J. Quantum Chem.* **29** 183–96
- Talbi D and Saxon R P 1988 *J. Chem. Phys.* **89** 2235–41
- Tennyson J 1982 *Chem. Phys. Lett.* **86** 181–4
- 1986 *Comput. Phys. Reports* **4** 1–36
- 1992 *J. Chem. Soc., Faraday Trans.* **88** 3271–9
- 1993 *J. Chem. Phys.* **98** 9658–68
- Tennyson J and Henderson J R 1989 *J. Chem. Phys.* **91** 3815–25
- Tennyson J and Miller S 1992 *Chem. Soc. Rev.* **21** 91–9
- 1994 *Contemp. Phys.* **35** 105–16
- Tennyson J and Polyansky O L 1994 *Phys. Rev. A* **50** 314–6
- Tennyson J and Sutcliffe B T 1984 *Mol. Phys.* **51** 887–906
- 1985 *Mol. Phys.* **54** 141–4

- 1986 *Mol. Phys.* **58** 1067–85
- Tennyson J, Brass O and Pollak E 1990a *J. Chem. Phys.* **92** 3005–17
- Tennyson J, Miller S, Henderson J R and Sutcliffe B T 1990b *Phil. Trans. R. Soc. London A* **332** 329–41
- Tennyson J, Miller S and Henderson J R 1992 *Methods in Computational Chemistry* vol 4, ed S Wilson (New York: Plenum) pp 91–144
- Tennyson J, Miller S and Schild H 1993 *J. Chem. Soc. Faraday Trans.* **89** 2155–9
- Tennyson J, Henderson J R and Fulton N G 1995 *Comput. Phys. Commun.* in press
- Thomson J J 1911 *Phil. Mag.* **21** 235–??
- 1912 *Phil. Mag.* **24** 209–53
- 1934 *Nature* **133** 280–1
- Tokunaga A T, Sellgren K, Smith R G, Nagata T, Sakata A and Nakada Y 1991 *Astrophys. J.* **380** 452–60
- Trafton L M, Carr J, Lester D F and Harvey P 1989a *Time Variable Phenomena in the Jovian System* ed M J S Belton, R A West and J Rahe (Washington: NASA) 229–34
- Trafton L M, Lester D F and Thompson K L 1989b *Astrophys. J.* **343** L73–6
- Trafton L M, Geballe T R, Miller S, Tennyson J and Ballester G E 1993 *Astrophys. J.* **405** 761–6
- Uy D, Gabrys C M, Jagod M-F and Oka T 1994 *J. Chem. Phys.* **100** 6267–74
- Van Dishoeck E F 1986 *Space-Borne Sub-Millimetre Astronomy Mission (Segovia, Spain)* pp 107–17
- Van Dishoeck E F, Phillips T G, Keene J and Blake G A 1992 *Astrophys. J.* **261** L13–6
- Varney R W 1960 *Phys. Rev. Lett.* **5** 559–60
- Ventrudo B F, Cassidy D T, Guo Z Y, Joo S, Lee S S and Oka T 1994 *J. Chem. Phys.* **100** 6263–6
- Warner H E, Conner W T, Petrmichl and Woods R C 1984 *J. Chem. Phys.* **81** 2514
- Watson J K G 1984 *J. Mol. Spectrosc.* **103** 350–63
- 1993 *J. Chem. Soc. Faraday Trans.* **89** 2170
- 1994 *Can. J. Phys.* **72** 702–13
- Watson J K G, Foster S C, McKellar A R W, Bernath P, Amano T, Pan F S, Crofton M W, Altman R S and Oka T 1984 *Can. J. Phys.* **62** 1875–85
- Watson J K G, Foster S C and McKellar A R W 1987 *Can. J. Phys.* **65** 38–46
- Watson W D 1976 *Rev. Mod. Phys.* **48** 513–52
- Wei H and Carrington T Jr 1994 *J. Chem. Phys.* **101** 1343–60
- Whitnell R M and Light J C 1988 *J. Chem. Phys.* **89** 3674–80
- 1989 *J. Chem. Phys.* **90** 1774–86
- Wigner E 1932 *Phys. Rev.* **40** 749–59
- Wilson E B Jr, Decius J C and Cross P 1954 *Molecular Vibrations* (New York: McGraw-Hill)
- Winnewisser G and Herbst E 1993 *Rep. Prog. Phys.* **56** 1209–73
- Wolniewicz L and Hinze J 1994 *J. Chem. Phys.* **101** 9817–29
- Wormer P E S and de Groot F 1989 *J. Chem. Phys.* **90** 2344–56
- Xu L-W, Rosslein M, Gabrys C M and Oka T 1992 *J. Mol. Spectrosc.* **153** 726–37